HIPPARCHOS

The Hellenic Astronomical Society Newsletter
Volume 3, Issue 3
ISSN: 1790-9252

Contents

HIPPARCHOS

Volume 3, Issue 3 • July 2020

ISSN: 1790-9252

Hipparchos is the official newsletter of the Hellenic Astronomical Society. It publishes review papers, news and comments on topics of interest to astronomers, including matters concerning members of the Hellenic Astronomical Society.

Contact person
Panos Patsis
Research Center for Astronomy & Applied Mathematics (RCAAM), Academy of Athens
Soranou Efessiou 4,
115 27 Athens, Greece
Tel: +30-210-6597-103
Fax: +30-210-6597-602
E-mail: patsis@academyofathens.gr

Printed by ZITI Publications • www.ziti.gr

Cover Image:
An NGC 1365 image (Credit: ESO. Acknowledgement: Aniello Grado and Luca Limatola), having in the background a room of a Supercomputing Center.

Message from the President

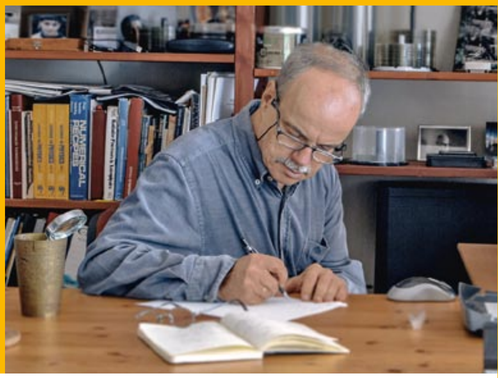

One thing is for sure: This last year will be one to remember and not for the best of reasons. The "normalcy" of life disappeared within a matter of days and this full scale collapse affected the Society as well. Trying to organize the HelAS elections amidst the pandemic proved a non-trivial task as we had to chose between various (bad) options. The delay of the date of the elections for one month was finally favored in order to give our members enough time to cast their votes by mail as we had information that mailing services were stalled and very few people would have been able to send their votes on time. On the other hand, delay of the elections until early autumn would have caused problems of bureaucratic nature. Therefore, once again, a middle road was taken. I think this is the first time that HelAS elections are delayed but "extreme situations require extreme measures" as the saying goes.

Another sobering event was the passing, after a long illness, of Prof. Yannis Seiradakis, who was the second President of our Society serving between 1998-2002. We have an obituary inside the present issue of Hipparchos but I would like to stress once more here that his contribution to the establishment of HelAS was invaluable. Eyewitness testimonies of the people who played a role in those early days tend to agree that it was him who had the vision of bringing Greek astronomers together in a Society. Not only that but he wrote the first draft of our statute and also made all the necessary contacts. As another past President, Prof. Paul Laskarides, wrote in a very informative note, Prof. Seiradakis was the *θρυαλλίς* of our Society but because of his modesty he never made this too obvious. I think that he succeeded thanks to his unique, nonchalant manner that made him so much liked by anyone who met him. Many things have been said and written during the last month, so I will simply say that he has set a paradigm with his high (and humane) standards in science, education and administration. A true gentleman. He will be sadly missed.

Well, life has to go on despite all and the present issue of Hipparchos is a testimony for that. It contains four very nice articles plus the usual conference reports and short news. The article of Dr. Yannis Zouganelis (European Space Agency) provides a very informative coverage of the Solar Orbiter mission, a joint ESA-NASA collaboration that was launched just a few months ago and hopefully will shed light to some of the Sun's best kept secrets like the origin of the solar wind, the solar dynamo and particle energization. Dr. Zouganelis, who is the Deputy Project Scientist of Solar Orbiter does not deal only with the science part of the mission but gives also a very informative look at the payload and the technological challenges which are, as one can imagine, on the extreme side as the satellite will get very close to the Sun. Overall the mission is an impressive achievement and I do hope that it will lead to some answers about our mysterious nearby star.

Prof. Lia Athanasoulla (Aix Marseille University) gives us a very personal review on how far numerical simulations have gone into helping us understand the way galaxies form and evolve using as a guide her own research on galactic dynamics from the early GRAPEs days up to present. The author touches upon many topics about galaxy formation and evolution and I find it overall a very enjoyable read because it shows, in the best possible way, that excitement should always be a part of good scientific research. Yes, science can be fun and research should be mentally rewarding as we get deeper and deeper inside our respective fields! I think that this is one of the key messages that we have to convey to the younger generations.

The article of Dr. Mirella Harsoula (Research Institute of Astronomy, Academy of Athens) is on a similar topic with the previous one dealing with the types of star orbits in spiral galaxies. This is rather on the technical side, yet it is clearly written and reviews nicely part of the substantial work performed on the topic by researchers in the Research Institute of Astronomy and their collaborators.

Last but not least Dr. Ioannis Myserlis (Instituto de Radioastronomía Milimétrica, Granada and MPIfR, Bonn) talks about linear and circular polarization in the jets of Active Galactic Nuclei. This is a rather difficult problem to tackle but the author does an excellent job as he starts from basic principles and then describes how a radiative transfer model that he built can help us decipher the observations and understand the physical conditions in the jets.

So by the time that you will be reading this I hope that everything will be moving back to normal and the elections will be very near. I also hope that the outgoing Governing Council has fulfilled its role at a time that not everything was business-as-usual. We had frequent and constructive meetings and I would like to thank everyone for their help. The new Council that will be formed after the elections will be of the highest caliber as it consists of young colleagues who are, in every aspect, on top of their form. I anticipate a further strengthening of the Society and, also, a few good surprises down the road. At such strange times that we all live in, this is something to look forward to. Stay safe.

Apostolos Mastichiadis
President of Hel.A.S.

In memoriam

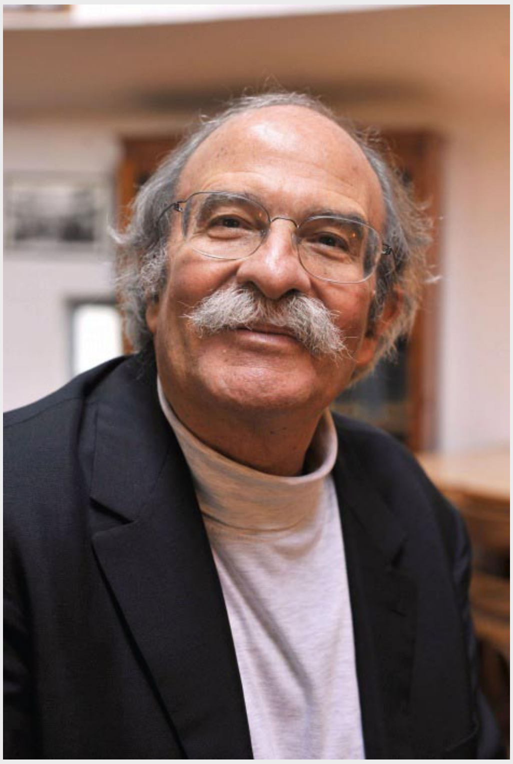

John Hugh Seiradakis (1948-2020)

With great sorrow we announce the passing of Prof. John Hugh Seiradakis, a respected and beloved colleague and professor and a founding member of our Society. John Hugh Seiradakis was not only the second President of our Society for four years (1998-2002), but he also masterminded its establishment and wrote the first document that eventually led to our Society's statute. In this respect Hel.A.S. can be considered as his brain-child.

John Hugh Seiradakis was born in Chania, Crete on March 5, 1948. He obtained his degree in Physics at the University of Athens (1971) and he continued his education at the Victoria University of Manchester, where he obtained his M.S. (1973) and his Ph.D. (1975) on the subject of pulsars observations under the supervision of Dr. John G. Davies.

He worked as a researcher at the Max-Plank Institut fuer Radioastronomie, Bonn, at the University of Hamburg and at the University of California, San Diego. In 1985 he was appointed Associate Professor at the Aristotle University of Thessaloniki and in 1996 he was promoted to full Professor. In 2011 he was elected Director of the Laboratory of Astronomy of the Aristotle University, a position that he held until his retirement in 2015, after which he was appointed Professor Emeritus. His domain of expertise included neutron stars, neutral hydrogen modeling in nearby galaxies, the center of our Galaxy, flare stars, Lunar Transient Phenomena and Archaeoastronomy. He has published more than 74 scientific papers in refereed journals and more than 80 papers in conference proceedings and special volumes, as well as three University-level textbooks. He has represented Greece in large European networks (OPTICON, ILIAS, CRAF, etc).

In December 2005, the highest EU prize Descartes was awarded to the Neutron Stars research network, “PULSE”, in which he was one of the founding members.

He was very active in promoting Astronomy to high school students and, in collaboration with the Society for Astronomy and Space at Volos, brought the best students to the International Olympiads of Astronomy and Astrophysics. He also promoted the science of Astronomy to the general public through conferences and popularized articles. Many of our colleagues discovered their inclination in Astronomy because of his inspiring and good-tempered personality. He will always be remembered by us all for his generosity, his leadership and for his selfless contribution to all things astronomical.

Studying galaxies with a computer: a brief overview

by **E. (Lia) Athanassoula**

Aix Marseille Univ, CNRS, CNES, LAM, Marseille, France
Corresponding member of the Academy of Athens, e-mail: lia@lam.fr

1. Introduction

At present, a very large number of opportunities are open to astronomers wishing to understand how galaxies form and evolve. Supercomputers allow them to make realistic, high resolution numerical simulations, including not only stars and dark matter, but also gas and its physics (star formation, different types of feedback, cooling, etc.), and chemical evolution, thus reaching full chemo-dynamics. On the observational side, a number of large surveys, of high resolution and sensitivity, provide data of unprecedented quality and quantity. The aim of this article is to 'wet the appetite' of young astronomers and incite them to work on the formation and evolution of galaxies, by providing as an example my own personal research experience in this field, and by describing how much fun such work can be. If I focus here on simulations and on observations, it is not because I look down upon analytic work. I simply consider such work as a *sine qua non*, an absolute necessity for any astronomer or astrophysicist, independent of the specific subject they work on. This was true in the past and continues to be true. I will here concentrate on the additional impact that the very strong recent advances in computational astrophysics can provide.

2. Orbits and gas flows in barred galaxies

Spiral arms in a galaxy are like icing on a cake, and can be treated as perturbations of the axisymmetric disc that hosts them. In my thesis work – done under the supervision and guidance of Professor George Contopoulos – I studied, mainly analytically, the spiral structure in the central parts of disc galaxies, introducing an extension of the density wave theory of Lin and Shu (1971), which at the time was a hot topic.

I obtained a job in France in the second half of the 1970s, and started using computational tools, enabling me to tackle a wider set of problems, beyond the linear regime mainly accessible to analytical studies. My first goal with these tools, which were new to me then, was to understand galactic bars. Indeed, these are much stronger features than spirals, and their dynamics is much more complex and challenging. I started by studying the motion of stars and gas in and around bars. For stars, considerable understanding was already available from periodic orbit studies (e.g. Contopoulos & Papayannopoulos 1980, Contopoulos & Grosbol 1989). I extended this work to potentials where the bar was described by a Ferrers model. For the gas flow, however, I needed an adequate, high quality hydrodynamic code (Van Albada & Roberts 1981, Van Albada, van Leer & Roberts 1982), with sufficient linear resolution to describe properly the shocks in the gas. With such a code and resolution, I could connect the shock loci in my simulations with the dust lanes on the leading sides of observed bars, and to show that their shape depends on many parameters, of which the most important ones are four, namely the mass, axial ratio and pattern speed of the bar, as well as the mass concentration in the central region.

An in-depth study of this kind necessitated a quite extended exploration of this four dimensional parameter space. Given the CPU speed of computers available at the time, this presented a serious difficulty, since high quality hydrodynamic simulations are very CPU time consuming. I was then working in the observatory of Marseille, which had a median sized computer, shared by many astronomers. As my codes were well optimised, they slowed down all data analysis more than could be accepted, so I was allowed to run my simulations only at night. Since two nights were needed for each run, it took well over a year to obtain sufficient results for a thorough analysis. However, the preliminary analysis I would obtain every morning from the previous night's results was sufficiently interesting to keep me going. Furthermore, since I used the same potentials for the orbital structure and the gas flow calculations, I could, at all stages of this endeavour, make many useful comparisons so as to understand the link between the main periodic orbits and the gas flow patterns, and to predict when shocks would form and what their shape and loci would be.

Two of my results excited me most. The first was that I could witness in my simulations how and when the gas is pushed inwards by the bar in order to form a nuclear ring, or move yet further inwards to form a central mass con-

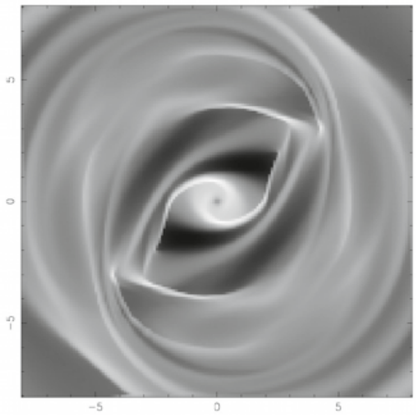

***Figure 1:** Gray scale plot of the gaseous response to a bar. Darker (lighter) shades correspond to lower (higher) densities. The bar rotates clockwise and its major axis is located along the NorthEast to SouthWest diagonal. Note that gas is concentrated in the central region and also in the shock loci along the leading side of the bar, while two extended regions on either side of the centre and near, or on, the bar have very low gas density. (This figure is reproduced from Fig. 10 in 'Unravelling the mystery of the M31 bar', by E. Athanassoula and R. Beaton 2006,* Monthly Notices of the Royal Astronomical Society, *vol. 370, Issue 3, p. 1499)*

centration and perhaps feed a central black hole. The second result was that my simulations set limits to the values of the bar pattern speed, a quantity difficult to obtain observationally. Within these limits, the shape of the shock loci reproduced well the shape of the observed dust lanes, while outside them this shape was unrealistic. Using the 225 simulations I had run, I could clearly say that the corotation radius, R_{cr}, had to be within the range (1.2 ± 0.2)a, where a is the length of the bar semi-major axis. The lower limit of this region was a confirmation of the result found earlier by Contopoulos (1980), relying on the structure of the periodic orbits, and of my own results on bar driven spirals. However, the crucial improvement that my gas flow calculations introduced was to set an upper limit to the corotation radius, i.e. a lower limit to the bar pattern speed, thus bracketing the allowable region. Even now, nearly 30 years later, this range is still considered as *the* comparison range for all observational and theoretical studies of bar pattern speeds (e.g. Cuomo et al. 2020, Guo et al. 2019, and references therein).

3. GRAPEs

My next aim was to study the formation and evolution of the bar component itself using a fully self-consistent simulation, i.e. one in which I could follow not only the evolution of the stellar disc, but also that of the dark matter halo. This was clearly beyond the limit that our 1980s observatory computer could handle, so I applied for time on the French supercomputers and started working on this subject. However, it became soon clear to me that, although I could make some useful progress on the subject, I was depressingly far from reaching my initial goal.

The next step was actually due to pure luck. Albert Bosma and I received a letter from Piet Hut from Princeton, telling us that a young and very promising Japanese student was touring the world, visiting a number of institutes, in an attempt to get a global view of international astronomy. Hut was asking us whether we could host this student for a few days. We were most happy to do so and a few weeks later Jun Makino was in Marseille. One of the things he talked about during his stay was a novel attempt his group in Tokyo University was making to solve the N-body problem, namely building a computer board which they called GRAPE (short for GRAvity PipE; Sugimoto et al. 1990).

Let me first give some necessary background, before describing what this board meant for us. In numerical simulations such as those I wanted to do, each component is described by a number of massive particles, e.g. the disc particles, the halo particles etc., which interact between them by gravitational forces. Calculating these forces takes up the vast majority of the simulation computer time. The idea behind the GRAPE is that these forces can be calculated by hardware, rather than software. Our Japanese colleagues built such a piece of hardware, which was linked to a front end computer sending it the particle positions. The board uses these positions to calculate the forces, and sends them back to the front end computer. I.e. the GRAPE board calculates only one thing, the forces between particles, but does this extremely fast because it has been specifically wired for it. This allowed one to have, albeit only for N-body simulations, a computing power equivalent to a Cray supercomputer, all to oneself and for little cost. Of course I wanted to have one on my desk!

The first GRAPE board we acquired was wired by hand, with a soldering iron, and thus had relatively limited capacities. Even so, plugged into our SUN workstation, it allowed us to familiarize ourselves with GRAPEs and with the associated computer language – as the software needed to operate such boards was not trivial – particularly for software such as the tree code. We then continued with more advanced GRAPE models with custom-made chips (GRAPE-3AF and GRAPE-4). We could do good science with these, while creating a small group around this project. The most interesting work we did with these first boards was a study of Hickson compact groups, i.e. relatively isolated groups of typically four or five galaxies, in close proximity to one another. Simple calculations, but also N-body simulations (e.g. Barnes 1989), had shown that the galaxies forming such groups should have already merged. The question we tackled is why in this case do we observe so many of them at low redshift. Why had the predicted mergers not occurred? The contribution of our team here was first to find how different halo radial density profiles influence the merging rates and then to find a profile for which the merging time is of the order of the Hubble time, thus providing a plausible solution to this problem. Except for this project, with our first GRAPEs we also modelled collisional rings such as in the Cartwheel galaxy, the formation of brightest cluster members and cD galaxies, the fate of bars during interactions and mergers, and the structure of cusps induced at the centre of elliptical galaxies by a super-massive black hole.

But the main breakthrough came with the GRAPE-5 boards, five of which we could acquire thanks to support from our main national funding agency, as well as help from our University and a regional government agency. My main collaborators here were A. Bosma and J. C. Lambert, but part of the initial work was also done by a bright Greek student, Angelos Misiriotis.

4. Bars

In the seventies and eighties I had been impressed by two seminal papers. The first one was by Lynden-Bell and Kalnajs (1972), who studied analytically the exchange of angular momentum within a spiral galaxy, focusing on the resonances and their role. The second one, about a decade later, was a paper by Tremaine and Weinberg (1984b, see also Weinberg 1985), who, mainly analytically, focused on how a spheroidal system, e.g. a halo, could absorb angular momentum at its resonances.

These two papers, together with the knowledge I had acquired on orbital structure in bars, led me to apply our quite considerable, GRAPE-based, computing capacity, to study in the nonlinear regime the role of individual resonances on bars and their evolution. This involved not only running fully self-consistent N-body simulations with very high resolution both for the disc and for its spheroids (i.e. the halo and the classical bulge), but also following the orbits during the simulation and studying their properties. My first step was to test the importance of the angular momentum exchange for the evolution of galaxies. For this, I compared the evolution of two simulated galaxies with initially identical discs (i.e. disc particles with the same positions and velocities), and spherical haloes with the same density distribution. The only difference between the two simulations was that in one of the two the halo was rigid – i.e. represented by a spherically symmetric, rigid, non-evolving potential which is not able to emit or absorb angular momentum – while in the other it was live, i.e. described by particles responding to any change in the disc and participating in the angular momentum exchange and redistribution. The difference between the two is stupendous (see Figure 2). In the first case no bar formed and the disc stayed roughly axisymmetric (rightmost panels), while in the second a very strong bar formed (middle panels). Just a single glance makes it clear that angular momentum exchange plays a major role in bar evolution. Hence, results from all simulations with rigid haloes should be taken with a pinch of salt, or rather simply discarded.

The next steps were less straightforward, because they implied understanding how the various resonances – whether in the disc or in the halo – worked, how the bar properties were linked to the angular momentum exchanged, and how various properties of the galaxy influenced this exchange. Guided by the analytical work, I could easily see that angular momentum is emitted at the inner Lindblad resonance within the bar region, and absorbed partly by the resonances in the outer disc, but also, and indeed mainly, by the halo resonances. This implies a major redistribution of angular momentum within the galaxy and a corresponding change of the bar, disc and halo properties with time. Thus, barred galaxies can never reach equilibrium, but keep evolving in time. The more angular momentum is exchanged, the stronger and longer the bar gets, while its pattern speed keeps decreasing. Such strong changes are found not only for bar properties, but also for those of other components of a galaxy.

While emphasising the angular momentum redistribution, simulations also established a further, even more important point. Namely, that barred galaxies must evolve continuously, and can never be stationary. Indeed, when a component or a region absorbs or emits angular momentum, its properties must change, both morphologically and kinematically. Since it is the bar that drives the angular momentum exchange and redistribution, we can say that it is the bar that drives this evolution. Compared to the changes brought by interactions and mergers, this evolution is quite slow, and is thus called secular evolution. It lasts several Gyr, i.e. much longer than interactions, and can influence the properties of disc galaxies as much, or even more than the latter.

Real galaxies are observed at one single time, and can, therefore, be compared only with specific snapshots in a numerical simulation sequence. Observations can thus produce only indirect evidence for secular evolution by testing for the evolution results, and I was happy to participate in a number of such works (see also Sect. 9). Secular evolution has also a strong influence on theoretical work, since many major problems cannot be tackled by time-independent dynamics, but need to take evolution properly into account.

Note that all this is in no way really new, as it simply confirms what was already discussed more than two thousand years ago by Heraclitus, as witnessed in his famous sentence "Ta panta rei" (in greek *Τα παντα ρει*).

The next step was to find which galaxy properties, preferably observable, may determine the amount of angular momentum exchanged. Even though I was to some extent expecting it, I was and still am flabbergasted by the complexity of this problem. Until then, the analytical or numerical calculations had shown that increasing the halo mass damped the bar strength in a model galaxy. It was thus thought that a halo is the worst enemy of a bar. Several papers discussed the amount of halo necessary to stop the bar from forming, or at least to slow it down sufficiently for no bar to form in less than a Hubble time (see e.g. the

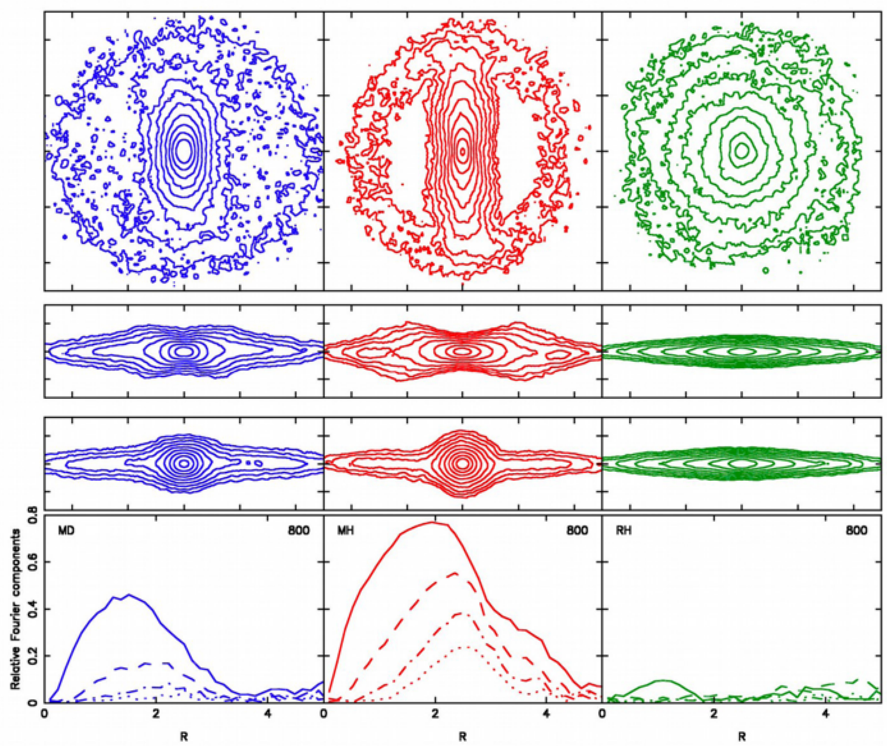

***Figure 2:** The effect of the halo on bar formation and evolution. From top to bottom: Isodensity curves of the face-on view of the galactic disc at the end of the simulation (first row), of the side-on view (i.e. edge-on, with the line of sight along the bar minor axis; second row), of the end-on view (i.e. edge-on, with the line of sight along the bar major axis; third row) and relative amplitude of the Fourier components m=2, 4, 6 and 8 of the density (with solid, dashed, dot-dashed and dotted lines, respectively; bottom row). Each column corresponds to a different simulation. The rightmost and the middle ones correspond to the same case, except that for the former the halo potential is rigid, i.e. does not participate in the angular momentum redistribution, while in the latter it is live, i.e. does participate. The difference is astounding. The left-most column is an intermediate case where the halo is live, but has been built so as to be able to absorb considerably less angular momentum. These three columns together argue strongly about the effect of the halo on the bar formation and evolution. (The three simulations of which we show some properties here were initially run for "Bar-Halo Interaction and Bar Growth", by E. Athanassoula, 2002,* The Astrophysical Journal, *vol. 569, p. L83.)*

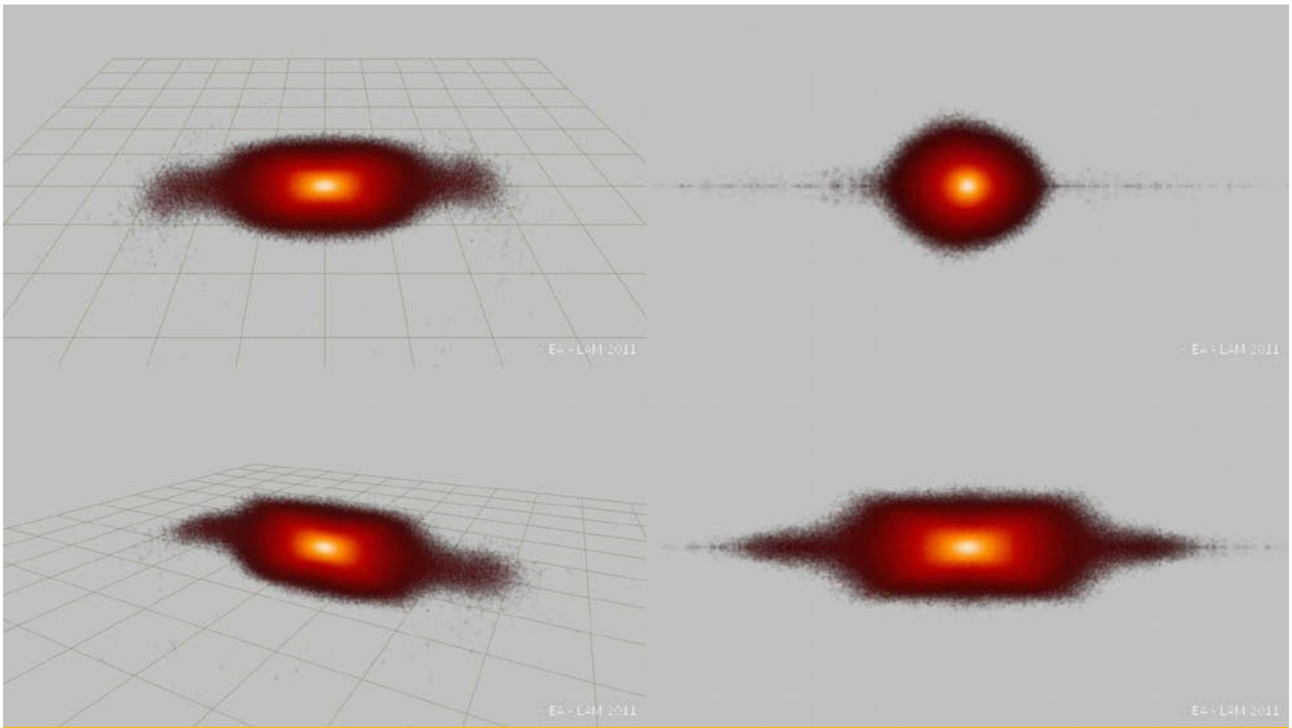

Figure 3: *Viewing the stellar bar from various angles. The right column gives a near end-on (upper row) and a near side-on (lower row) view. The left column gives two viewings from intermediate angles, which can be estimated from the cartesian grid on the bar equatorial plane. All viewings show that the inner part of the bar is considerably thicker than the outer part, i.e. that not the whole of the bar is vertically thick, only its inner part, which is also known as the boxy/peanut bulge. (The lower right panel is taken from the upper panel of Fig. 1 in "Modelling the inner disc of the Milky Way with manifolds – I. a first step ", by M. Romero-Gomez, E. Athanassoula, T. Antoja and F. Figueras 2011,* Monthly Notices of the Royal Astronomical Society, *vol. 418, Issue 2, p. 1176.)*

classical paper by Ostriker & Peebles 1973).

I could, however, clearly see in my simulations that this is true only in the initial, linear stages of the simulation, while later on, after the bar has sufficiently grown and the problem has become strongly nonlinear, the halo will help the bar grow, as it absorbs the angular momentum emitted by the bar. The more massive the halo, the more angular momentum it can absorb and the more the bar will grow. But the mass of the halo is not the only relevant quantity. Its central concentration, its mean rotation and its velocity dispersion also influence the amount of angular momentum the halo can absorb. To this, one must add quantities that affect the mass and the velocity distribution in the disc resonant regions, the existence and properties of the classical bulge, those of the thick disc, etc. etc. I will not bore the reader with discussions of these numerous properties or quantities influencing bar formation and evolution, which have been the subject of many papers, while more are still to come. I will only mention that, as with all problems where the relevant parameter space has many dimensions, it is exceedingly difficult, if at all possible, to use the strength or the pattern speed of the bar to set limits on the values of relevant parameters, such as the halo mass, or shape.

So far I have given only a 2D view of bar formation and evolution. But the formation of bars due to a disc instability is only a beginning. A further instability occurs after a bar forms, because some of the bar orbits become vertically unstable. As a result, some simple, planar, elliptical-like bar orbits jump out of the galactic plane and take the shape of a smile, or a frown. Hence part of the bar thickens vertically and protrudes out of the galactic plane, taking the form of a box, or of a peanut, and becomes the so-called boxy/peanut bulge. The knowledge of orbital structure now becomes indispensable, since it allows us to understand the complex shape of bars, based on the vertical stability or instability of families of periodic orbits.

All the above results rely on a very large number of high resolution simulations, i.e. required a lot of CPU time, which can be obtained only with parallel supercomputers and/or new types of software (e.g. Dehnen 2000, 2002). Thus the GRAPEs were gradually phased out. This became definite when it was realized that in order to understand many aspects of secular evolution it was necessary to include the gaseous component and its physics in the simulations. The behaviour of gas in galaxies is not easily described by a simple code which can be hardwired onto a computer chip.

5. Bars in yet more realistic models

In collaboration with R. Machado and S. Rodionov, I undertook two further steps which were necessary in the quest for realistic bar formation and evolution scenarios in simulations. The first one concerned the shape of the dark matter halo component, which had been, in most previous studies, considered as spherical, for simplicity. It was clear, however, that gravitational interactions with other galaxies could alter this shape, as is also shown by cosmological simulations. In cases with triaxial haloes, the galaxy will have two non-axisymmetric components, the bar and the halo, both of which can exert torques, so that angular momentum can be redistributed within the galaxy.

We found that the triaxiality of the halo has two different effects. In the early stages, when the bar just starts forming, a non-axisymmetric halo and its torque incite the bar to form earlier. At later stages, however, and, more specifically during the secular evolution phase, the halo non-axisymmetry in general damps bar growth.

These simulations are even more realistic because they include gas and its physics, i.e. star formation, feedback and cooling. They showed that, when all the remaining galactic properties are the same, a more massive gaseous component makes the stellar disc stay near-axisymmetric over longer times than a less massive gas component. Furthermore, in such gas rich galaxies, when the bar starts to grow, it does so at a much slower rate. This predicts that bars should be in place earlier in massive red disc galaxies than in blue spirals, in good agreement with what has been observed (see Sect. 9).

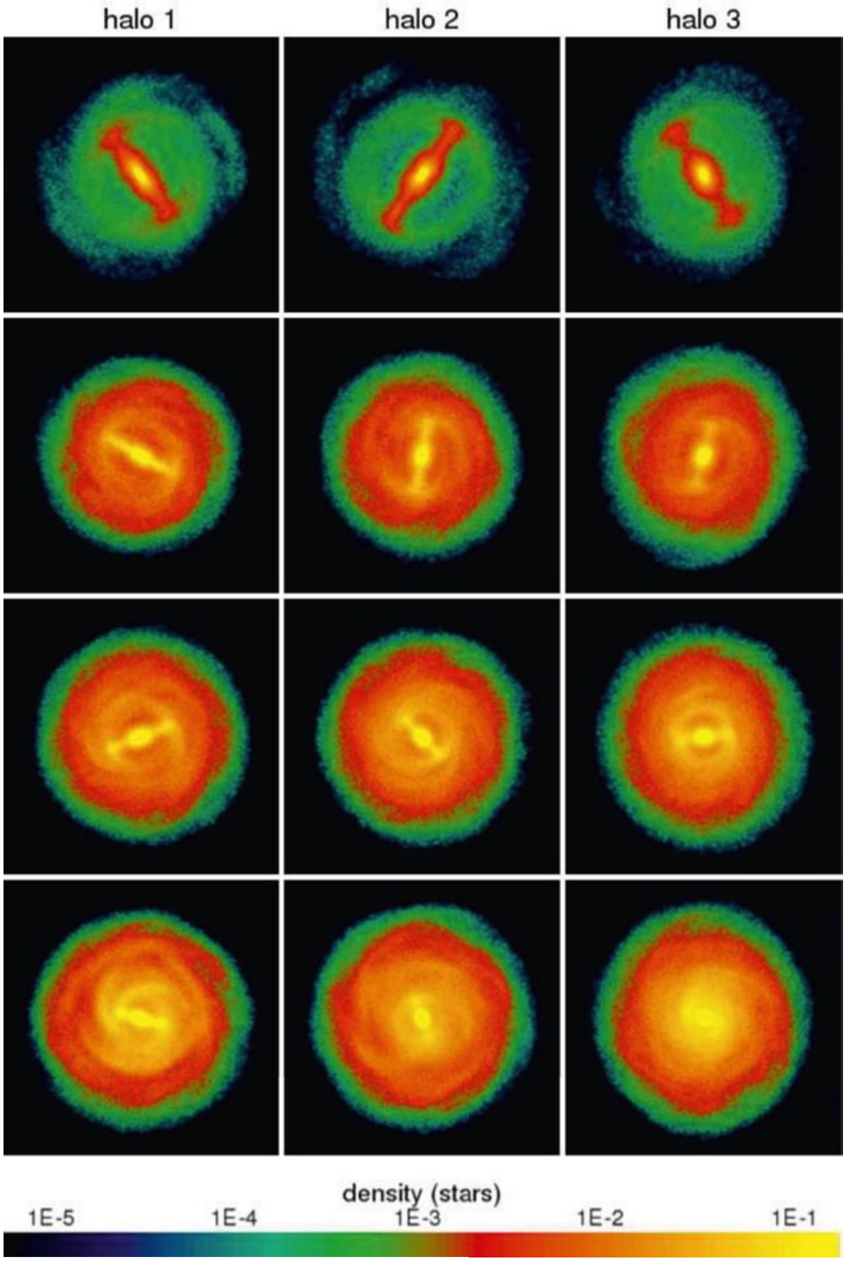

Figure 4: *Face-on view of the stellar population in twelve simulations with different initial gas fractions and dark matter halo shapes. From top to bottom, the various rows correspond to an initial gas fraction of 20%, 50%, 75% and 100%, respectively. From left to right the three columns correspond to spherical, somewhat triaxial, and strongly triaxial dark matter haloes. Rotation is counterclockwise. Colour represents projected density and the corresponding numerical values are given by the colour bars in the bottom of the figure. The size of each square box corresponds to 40 kpc. (This figure is part of Fig. 5 in 'Bar formation and evolution in disc galaxies with gas and a triaxial halo: morphology, bar strength and halo properties', by E. Athanassoula, R. E. G. Machado and S. A. Rodionov, 2013,* Monthly Notices of the Royal Astronomical Society, *vol. 429, Issue 3, p. 1949.)*

6. Forming discs in mergers

In scientific research a question often leads to a result, which, in turn, leads to another question. So, after having spent several years on trying to understand the formation and evolution of bars with the help of N-body simulations, I found myself wondering whether the standard approach followed by dynamicists was the right one. The initial conditions in these numerical simulations are a disc in quasi-equilibrium in its host halo, so that, dynamically, the problem is well set. But is this how bars form in real galaxies? Does a disc form first in its halo, and then evolve to an axisymmetric equilibrium which is bar unstable, so that bar formation starts? Was the disc always bar-stable as it grew to an axisymmetric equilibrium? Moreover, could it be that by starting in such a quiescent way, we bias our results? To try and answer such questions I had to take a step back and start thinking about how discs may have formed.

Obtaining an even simplified and schematic view about this is far from trivial. We know that there are a number of mergers even in the local Universe, and that their number increases strongly as we go further back in time. So I thought of trying to use these mergers to create disc galaxies.

In the seventies, Alar Toomre had presented mergers as a possible way of creating elliptical galaxies, thereby introducing the notion that a merger does not necessarily lead to a messy heap of stars, but to another galaxy, presumably of a different kind (Toomre & Toomre 72, Toomre 77). Although this picture was initially heavily criticised[1], it gradually got adopted after both obser-

1. Gerard de Vaucouleurs once remarked that "after a collision a car is a wreck, not a new type of car!"

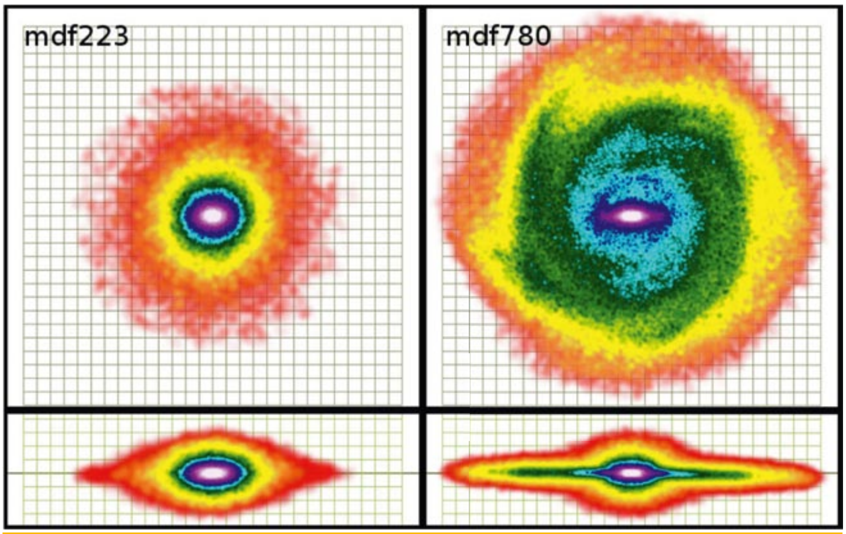

Figure 5: *The effect of a hot gaseous halo in disc galaxy formation. Comparison of two simulations, one with (right panels) and the other without (left panels) a hot gaseous halo, both at time t=10 Gyr. The upper and lower panels show the face-on and edge-on views, respectively. The Cartesian grid included in the background has cells of 1×1 kpc size. (This figure is part of Fig. 8 in "Forming Disk Galaxies in Wet Major Mergers. I. Three Fiducial Examples", by E. Athanassoula, S. A. Rodionov, N. Peschken and J. C. Lambert, 2016,* The Astrophysical Journal*, vol. 821, article id 90.)*

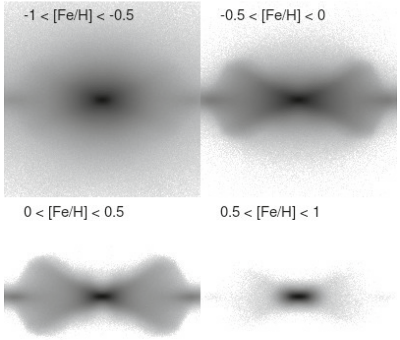

Figure 6: *Bar/bulge region viewed side-on to the bar, separately for stellar groups of different metallicity. This increases from left to right and from top to bottom, and one can see it roughly as an age sequence. Note that the distribution of the oldest stars (top left panel) is roughly a triaxial ellipsoid, not reminiscent of the side-on shape of the bar. The second group (top right) shows clearly a peanut/X shape, but looking carefully one can see the ellipsoid of the older stars, as well as part of the disc. The latter has disappeared from the next group (bottom left), while the youngest group (bottom right) must presumably be mainly the discy pseudo-bulge. (This figure is reproduced from Fig. 3 in "Metallicity-dependent kinematics and morphology of the Milky Way bulge", by E. Athanassoula, S. Rodionov and N. Prantzos 2017,* Monthly Notices of the Royal Astronomical Society*, vol. 467, Issue 1, p. L46.)*

vations and simulations came up with results that argued in its favour. Many of the simulations following this seminal work included gas, and a number of them showed some disc formation. The resulting disc, however, is too small and insufficiently massive, much less so than the large and very massive classical bulge at the galaxy centre. Thus, such simulations never formed any proper disc galaxy. There were strong hints that by increasing the gas fraction in the two colliding galaxies one got a better disc component, but even unrealistically high gas fractions proved insufficient.

I was about to give up this line of thought, when I saw some light at the end of the tunnel. I realised that the main problem was that, during the merging, the gas was pushed inwards to the innermost regions, where its density reached high levels and triggered very strong bursts of star formation. Thus the gas was consumed and could not form a decent disc. This explained why all these trials with very gas-rich progenitors could not form proper disc galaxies. Hence what was necessary was some gas that would escape this fate and rain in after the main star formation burst. If I was making this chain of thoughts today, it would be obvious how this gas would come in. But at that time relatively little was known about the circumgalactic medium, so I lost quite a bit of time pondering about whether this was a reasonable path to follow.

To understand this fully, S. Rodionov and I ran two simulations, both starting with a pair of two protogalaxies. In the first simulation, the two protogalaxies had a hot gaseous halo each, while in the second one this gas was replaced by dark matter particles (to keep the dynamics of the two cases as similar as possible). The stellar component of the remnant is shown in Fig. 5, with the first simulation to the right and the second to the left. The effect of the circumgalactic gas in disc formation became now quite clear at a glance. The merger remnant of the simulation with circumgalactic gas has an extended thin disc with realistic structures, such as a bar and spiral arms, while the one without this gas had a short, low mass disc with practically no structure. Viewed edge-on the former shows a realistic bulge outline and an extended thin disc component, both of which are clearly absent from the latter (see Fig.5).

Of course a lot of work was still necessary to show that the merger remnant can have properties that are in agreement with the main properties of observed disc galaxies. My collaborators in this endeavour are S. Rodionov, A. Bosma, N. Peschken and J. C. Lambert. We still have not completed all this, but we have found a lot of very encouraging results and, most important, a number of very good agreements with observations. Here is a partial list: The radial density profiles of the discs are exponential and have a break, which in most cases is type II (i.e. downbending compared to the inner disc), although there are also type III profiles (i.e. upbending compared to the inner disc). The disc has two components, a thin and a thick one. A classical bulge, as well as a fair part of the thick disc, is formed from the stars born before the merging, so that at the end of the simulations, i.e. around redshift zero, the classical bulge and the thick disc contain on average older stars than the thin disc. Boxy/Peanut bulges as well as discy pseudo-bulges and classical bulges formed in many cases, sometimes all three in the same simulated galaxy. The properties of the bars and the spirals that formed in these discs are also quite encouraging.

More recently, we coupled the chemical evolution code of N. Prantzos to the code we use to follow the dynamical and hydrodynamical evolution, which opened yet further perspectives. In particular, it allows us to set tighter constraints on the models, using age, metallicity and alpha-element radial profiles. We showed that in the central region of the Galaxy, known as the bar/bulge region, cohabitate a number of components, such as the stellar halo, the various types of bulges (classical, discy, and boxy/peanut), the thin and the thick disc, and their corresponding bar components. Each of these has its own morphology, kinematics and dynamics. It is thus a very complex, but very interesting region to study, and the results can now be compared with detailed observations provided by Gaia, and related surveys of various types of stars in the Milky Way.

7. Dark matter halo

The dark matter halo can not be directly observed as it does not emit in any observable wavelength. Thus, our knowledge of its properties is severely limited. We can, nevertheless, study it indirectly from the effects it has on other components, which we can observe. Therefore, the main tool with which we can obtain information on this halo is galaxy dynamics. The basic approach is very easy to understand. The velocities of stars and/or gas can be observed as these are constituted by baryons. We can then use dynamics to calculate the part of these velocities that is due to the gravitational forces of the baryonic distribution. Whatever can not be accounted for by the baryons must come from the dark matter. In this way we can obtain constraints on the amount and distribution of the dark matter mass assuming that the forces are Newtonian. More recently, other laws of gravity have started being explored.

It is also possible to use more elaborate dynamics. For example, in an early collaboration with A. Bosma and S. Papaioannou, I used constraints introduced by the swing amplification theory of spiral structure (Toomre 1981). Assuming that this theory can indeed explain the formation of spirals in observed galaxies, we reached some useful conclusions on the dark matter haloes in nearby disc galaxies.

Given the importance of dark matter in all galactic dynamics, I also participated in a number of studies aiming to detect it. The first one considered the effect of the halo shape on the dark matter annihilation signal expected from a weakly interacting massive particle (WIMP) in the region of the Galactic centre. In a second study, we estimated the gamma ray and neutrino fluxes coming from dark matter annihilation in a Milky Way framework using a Milky-Way-like, cosmological N-body simulation. We also used a cosmological simulation which includes baryons to study the dark matter direct detection signal. Although the results of all these attempts gave useful constraints, they are only a very minor step and much more effort is necessary before we have a definite solution to the dark matter problem.

8. Orbital structure

If one wants to build a house, one must first consider what bricks and other components to use. In the same way, in order to understand how a galaxy forms and evolves, one must first study the orbits of the stars that constitute it. This is a fascinating part of dynamics, as it can reveal many interesting aspects of galaxies. Two questions attracted me most:

The first question, on which I worked mainly in collaboration with P. Patsis and Ch. Skokos, is how orbits can get together to form the thin and the thick part of bars. Simple straightforward studies of periodic orbits can provide answers to crucial questions such as: what sets the limits to the extents of bars? Why are the inner parts of the bar thick, in contrast to the outer parts that are thin? Why don't we observe bars that, in their face-on view, have a major to minor axis ratio smaller than a certain limit? What is the role of chaos in forming bars? etc. etc.

The second question, on which I worked mainly in collaboration with M. Romero-Gomez, is whether spirals in barred galaxies can be due to manifolds. At first sight this might seem incongruous, as manifolds are linked to chaos, while spirals are thin, well defined structures with clear limits. This, however, is a too hasty conclusion, since the manifold driven orbits are spatially guided by their manifolds and therefore able to outline structures. The corresponding chaos is often referred to as 'confined chaos'. Manifold theory is relatively simple, relying on the dynamics of the Lagrangian points of the bar, and has had many successes. It can account both for spirals and for inner/outer rings, and the thus formed outer rings have the observed R1, R'1, R2, R'2 and R1R2 morphologies, as well as the dimples near the direction of the bar major axis. It also explains why the vast majority of spirals in barred galaxies are two armed and trailing, and naturally comes to the conclusion that stronger bars will create more elongated rings.

9. Observations

My husband is also an astronomer, doing observations at many different wavelengths. Thus, I learnt very early-on that a theory which does not compare reasonably well with observations, even if it is very elegant and mathematically correct, is of little use.

The first large scale collaboration that he and I were invited to join together was the S^4G (Spitzer Survey of Stellar Structure in Galaxies, Sheth et al. 2010). This is a survey comprising images of roughly 2400 galaxies taken by the Spitzer space telescope at 3.6μm and 4.5μm, i.e. the wavelengths where mainly the older stars emit. Since these stars contribute the bulk of the baryonic mass in galaxies, they can provide information which is essential for understanding galactic dynamics and evolution.

The S^4G group consisted of about three dozens astronomers, covering with their expertise all the necessary fields. Of major importance is the fact that this group found from the very start optimum ways of collaborating,

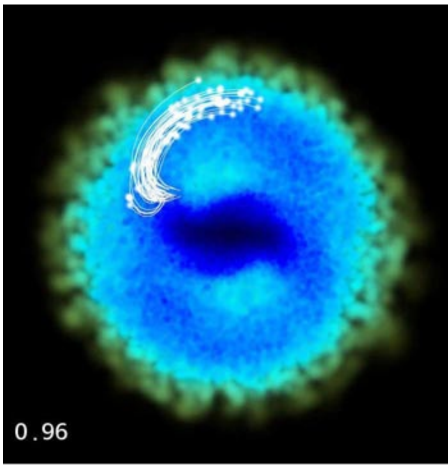

Figure 7: *Disc component in a simulation snapshot, on which are overlaid the locations (white filled circles) and trajectories (white solid lines) of a representative set of particles. Note how the latter trace the spiral arm. (This figure is the middle row, left column panel of Fig. 4 in 'Manifold-driven spirals in N-body barred galaxy simulations', by E. Athanassoula, 2012,* Monthly Notices of the Royal Astronomical Society, *vol. 426, p. L46.)*

leading to a very large number of interesting results, on a wide variety of subjects such as the galaxy stellar mass, its morphology, the thick disc, bars, spirals, rings, disc breaks, secular evolution, links with environment, studies of individual galaxies, etc.

The study of the structure of our Galaxy is now being revolutionized, thanks to the Gaia satellite, and the related ground-based spectroscopic surveys. I was involved in a number of such works, and particularly in the ARGOS survey (Ness et al. 2013, and references therein) which gave us the kinematics, metallicity and alpha enhancements of about 28000 stars in the bulge region and out into the thick disc. We first sought the origin of the split red clump in the Galactic centre and linked it to the boxy/peanut shape of the Galactic bar. This, together with our kinematics and metallicity results, demonstrated that the Galactic bulge is most likely due to internal dynamical processes, rather than mergers. Using a simulation which includes the various stellar populations in the bar/bulge region we reproduce very adequately the observed velocity dispersion profiles with longitude and their variations with galactic latitude and metallicity of the populations (see Sect. 6 for more information).

In extragalactic astronomy, the main new optical instruments are integral field spectrographs, and many surveys such as CALIFA, MaNGA and SAMI are already delivering 3D (2D spatial and 1D spectral) kinematic information from the gaseous and stellar components. The precursors of the SKA (Square Kilometre Array) radiotelescope, doing 21-cm HI line imaging and kinematics, are just entering this phase. Here also I am part of a number of collaborations, to which I contribute mainly in the modelling and interpretation of the data. In collaboration with a large team from several countries, we used MaNGA data and the Tremaine-Weinberg method (1984a) to get estimates of the bar pattern speed for a large number of barred spirals and compared them with those from simulations. Other collaborations focused on star formation in the centres of galaxies, trying to understand why this can be very strong in some cases, and very low in others, or trying to establish the role of bars and of interactions using data from CALIFA and EDGE. This list is far from complete, but gives some feeling of the many possibilities that are now available.

In order to understand the formation and evolution of bars better, I also participated in a few studies of galaxies at higher redshifts. I was a member of a large team from various countries, headed by K. Sheth, which, using the 2 square degrees COSMOS data set (Sheth et al. 2008), found that the fraction of spiral galaxies that have a bar component is a strongly declining function of redshift. We further found that the bar fraction depends also on the galaxy stellar mass, integrated colour and bulge prominence. In very massive, luminous spirals the fraction that is barred is roughly constant out to $z \sim 0.84$, while for the low-mass, blue spirals this fraction decreases considerably with redshift beyond $z = 0.3$.

10. In way of a conclusion

It is usual to end such articles by some conclusions. I will not do that because this is a subject in which every end is just another beginning. But I can definitely bring up a few points.

The first is that it is great fun to work on galaxies, their structure, dynamics, formation and evolution. In this field of research, there are so many very interesting and yet unanswered questions, for which a lot of information is available and awaiting eager minds.

The second is that this is indeed a very good time to study galaxies. Observational data in many wavelengths, covering morphology, kinematics and photometry, are publicly available and awaiting to be modelled and understood. Moreover, computer hardware, with several thousands of processors working in parallel, and coupled to the appropriate software, allows us now to explore questions which, not too long ago, would be only considered as in the realm of science fiction. So this is the moment to work on galaxies and if any young student is looking for an exciting thesis subject, my advice to them would be to consider galaxies, their formation and evolution!

Last but not least, this is a subject for which it is very useful to have a relatively broad view. The best is to repeatedly ask oneself how the specific thing one is concentrating on at the time fits in the general picture. This allows one to make links which had not been noticed before and stops one from devoting too much time to things which are secondary. Furthermore, it is a strong asset to be able to choose from a wide spectrum of 'tools' the ones that are most appropriate for tackling the problem at hand. Such 'tools' can range from theoretical techniques, to state-of-the-art numerical simulations, to data from large available observational surveys and to data reduction and visualisation tools. It is always refreshing to try a new field or a new technique.

Good luck in your quest for understanding galaxies. You will find it good fun, so be sure you enjoy every minute of it.

References

Barnes, J. 1989, *Nature*, 338, 123

Contopoulos G. & Papayannopoulos T. 1980, *A&A*, 92, 33

Contopoulos G. 1980, *A&A*, 81, 198

Contopoulos G. & Grosbol P. 1989 *A&ARv*, 1, 261

Cuomo V. et al. 2020, arXiv:2003.07455

Dehnen, W. 2002, *J. Comp. Phys.*, 179, 27

Dehnen, W. 2000, *ApJ*, 536, 39

Guo, R. et al. 2019, *MNRAS*, 482, 1733

Lin, C. C. & Shu, F. 1971, in "Astrophysics and general relativity", 2, 235

Lynden-Bell, D., Kalnajs, A. J., 1972, *MNRAS*, 157, 1

Ness, M. et al. 2013, *MNRAS*, 432, 2092

Ostriker, J. P. & Peebles, P. J. E. 1973, *ApJ*, 186, 467

Sugimoto D. et al. 1990, *Nature*, 345, 33

Sheth, K. et al. 2008, *ApJ*, 675, 1141

Sheth, K. et al. 2010, *PASP*, 122, 1397

Toomre, A., & Toomre, J. 1972, *ApJ*, 178, 623

Toomre, A. 1977, in "The Evolution of Galaxies and Stellar Populations", eds. B. M. Tinsley & R.B. Larson, Yale University Observatory, p. 401

Toomre, A. 1981, in "The structure and evolution of normal galaxies", Cambridge University Press, 1981, p. 111

Tremaine, S. D., Weinberg, M. D. 1984a, *ApJL*, 282, 5

Tremaine, S. D., Weinberg, M. D. 1984b, *MNRAS*, 209, 729

van Albada, G. D. & Roberts, W. W., Jr. 1981, *ApJ*, 246, 740

van Albada, G. D., van Leer, B. & Roberts, W. W., Jr. 1982, *A&A*, 108, 76

Weinberg M. D. 1985 *MNRAS*, 213, 451

The building blocks of spiral arms in galaxies

by **Mirella Harsoula**
Research Center for Astronomy, Academy of Athens

I. Abstract:

Spiral galaxies make up a very large proportion of all the galaxies in the Universe. Hubble classified the galaxies, in 1926, into ellipticals and spirals and divided the latter into two subcategories (Figure 1). Morphologically, about two-thirds of spiral galaxies present a bar in their center and are called barred spiral galaxies. The rest of the spiral galaxies have no bar and either they present well defined spiral arms (called "grand design galaxies" which usually have two well defined spiral arms), or they present multi-arm and flocculent spirals which have subtler structural features.

We investigate the types of the orbits of the stars that form the building blocks of the spiral arms in the case of the "grand design" galaxies as well as in the case of the barred spiral galaxies (like the Milky Way). In the case of the grand design galaxies with no bar, organised elliptical orbits can create a density wave in a spiral form. We give such an example of an analytical galactic model and we investigate the dependence of this spiral density wave on the amplitude of the pertubation of the model and the pattern speed of the spiral arms. On the other hand, in the case of spiral galaxies with bar, the density perturbation of the bar, in relation with the axisymmetric backgroud, is so large that there exist no more organised orbits that can support the spiral arms. For this type of galaxies the dominant theory for the formation of the spiral structure, nowadays, is the "manifold theory" introduced in 2006 according to which chaotic orbits with initial conditions along the unstable manifolds of unstable periodic orbits in the vicinity of the corotation, as well as sticky chaotic orbits close to the previous ones can support the spiral structure of the galaxy for long enough times before they go too far. We give such an example of a Milky-Way like barred spiral galaxy and we reconstruct the spiral structure using the chaotic orbits described above.

II. Introduction

Before the foundation of the density wave theory, the astronomers believed that the spiral arms of galaxies consisted of the same stars all the time. However the stars that are closer to the center of the galaxy move faster than the stars that are at the edge of the galaxy and so with the passage of time the spiral arms would become tighter (Fig. 2). This is something that is not observed in real galaxies and it is known as the "winding problem". This problem made astronomers finally understand that the spiral arms are areas of great density and do not consist continuously of the same material.

The density wave theory was introduced by Lindblad (1940, 1961), while later on Lin and Shu (1964) suggested that the spiral arms are created from density waves that survive for long enough time on the galactic disc. These spiral density waves have density perturbation up to 10-20% relative to the axisymmetric background

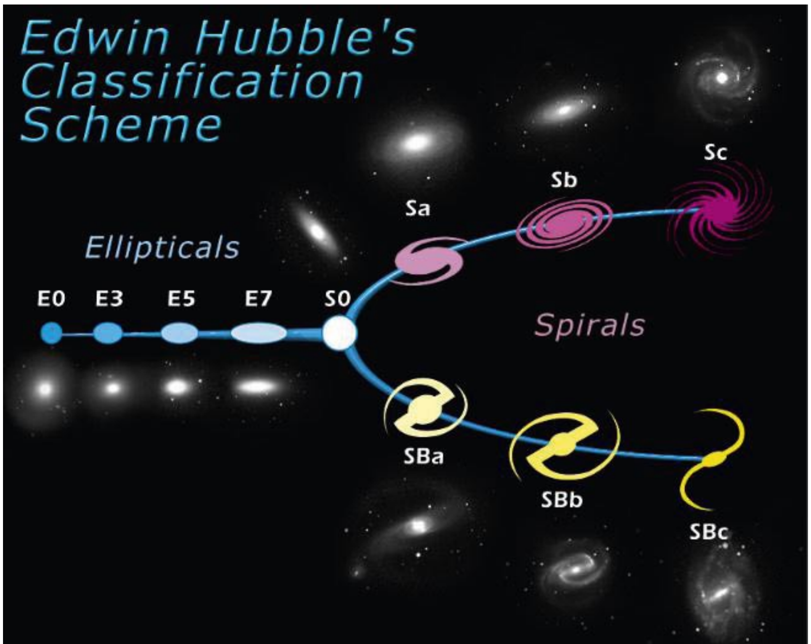

Figure 1: *The morphological categorization of galaxies given by Edwin Hubble in 1926.*

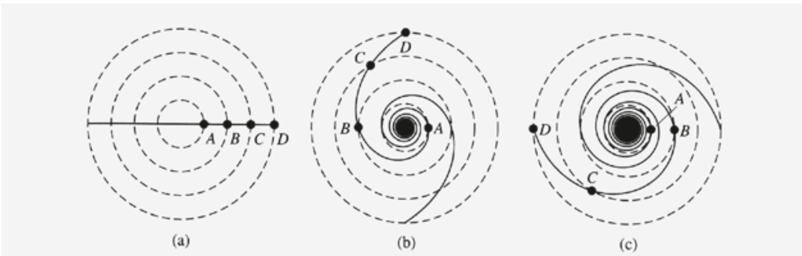

Figure 2: *The "winding problem" of galaxies. Stars that are closer to the center of the galaxy move faster than the stars that are at the edge of the galaxy. So, if spirals were made of the same material all the time, they should become increasingly tighter.*

and turn on star formation. Stars, gas and dust travel through these waves. Nevertheless, most of the stars do not have the same angular velocity with the wave. Stars that move inside corotation (the radius where the stars and the density wave have the same angular velocity) have greater angular velocity than the speed of the wave while stars moving outside corotation have smaller angular velocity than the one of the wave.

The existence of elliptical periodic orbits is very important for the support of the bar in barred spiral galaxies as well as for the support of the spiral structure in the "grand design" galaxies. In the case of "grand design" galaxies (without a bar) the regions close to the apocenters of such elliptical orbits, change with the energy in such a way that they can support spiral density waves to a large extend. These "precessing ellipses" were first designed schematically by Kalnajs (1973) and form the orbital version of the original Lin and Shu density wave theory. The change of the orientation of the elliptical orbits with the energy is explained by the perturbation theory in the case of the Inner Lindblad Resonance (ILR) (see Contopoulos 1975). Numerical examples of such precessing ellipses have been done in self-consistent models of spiral galaxies (Contopoulos and Grosbol, 1986, Patsis et al. 1991).

While in the case of grand design spiral galaxies the non-axisymmetric perturbation is small, of the order of 10% or even less (and therefore chaos is not important for the disc dynamics), in the case of barred spiral galaxies the non-axisymmetric perturbation can reach a value more than 50%. Therefore, in the latter case, chaos becomes very important and there are no more regular periodic orbit that can support the spiral structure. A new theory prevailed for this case, introduced by two different groups (Voglis et al., 2006 and Romero-Gomez et al., 2006), called "manifold theory". According to this theory the spiral arms of the barred spiral galaxies are supported by chaotic orbits having initial conditions along the unstable asymptotic manifolds of the unstable periodic orbits around the Lagrangian points L_1 and L_2.

III. Density waves in grand design spiral galaxies

In the paper of Contopoulos and Grosbol (1986) the authors mentioned the special importance of the "central family" of periodic orbits in galactic models. These orbits emanate from the stable circular orbits in the case of an axisymmetric galactic model. By adding a perturbation of a bar or a spiral potential, these orbits are deformed and they become elliptical. This ellipticity can become large enough if the non-axisymmetric perturbation has a large value. Nevertheless, for a relatively small perturbation of the galactic potential, like in the case of grand design galaxies that possess no bar, these deformed ellipses are still stable orbits. This means that they can trap matter around them and thus they can support the galaxy morphology. An example of such a 2-D analytical galactic model that simulates a grand design spiral galaxy is given below. This model consists of a galactic disc, a halo, a central spheroidal (bulge) and a logarithmic spiral potential. The total galactic potential is given by the relation:

$$V = V_{ax} + V_{sp} \tag{1}$$

where V_{ax} is the axisymmetric potential:

$$V_{ax} = V_d + V_b + V_h \tag{2}$$

which consists of a disc potential V_d, a central spheroidal (bulge) potential V_b and a halo potential V_h. More analytical, the disc potential V_d is a Miyamoto-Nagai (Miyamoto and Nagai, 1975) potential given by the relation:

$$V_d = \frac{-GM_d}{\sqrt{r^2 + \left(ad + \sqrt{z^2 + bd^2}\right)^2}} \tag{3}$$

where M_d = 8.56×10^{10} $M_\odot$ is the total mass of the disc ad = 5.3kpc and bd = 0.25kpc. In order to have a 2-D disc model we take z = 0. For the bulge we use a Plummer Potential V_b given by the relation:

$$V_b = \frac{-GM_b}{\sqrt{r^2 + b^2}} \tag{4}$$

where M_b = 5×10^{10} $M_\odot$ is the total mass of the bulge, $r = \sqrt{x^2 + y^2}$ and b = 2kpc. Finally, V_h is the halo potential introduced by Allen and Santillan (1991) and is given by the relation:

$$V_h = \frac{-GM_h}{r} - \frac{GMh_0}{\gamma r_h}\left[-\frac{\gamma}{1+(r/r_h)^{\gamma}} + \ln\left(1+(r/r_h)^{\gamma}\right)\right] \tag{5}$$

where γ = 1.02. The mass inside the radius r is given by the relation:

$$M_h(r) = \frac{M_{h0}(r/r_h)^{\gamma+1}}{1+(r/r_h)^{\gamma}} \tag{6}$$

with $M_h(r) = 10.7\times10^{10}\,M_\odot$

and $r = \sqrt{x^2+y^2}$.

The potential of the spiral arms is given by a logarithmic relation that simulates the spirals of our galaxy and is introduced by Cox and Gomez (2002):

$$V_{sp} = 4Gh_z\rho_0 \exp\left(-\left(\frac{r-r_0}{R_s}\right)\right)\frac{C}{KD}\cos\left(2\left[\varphi - \frac{\ln(r/r_0)}{\tan(a)}\right]\right) \tag{7}$$

where $C = 8/(3\pi)$,
$h_z = 0.18\,kpc$ $r_0 = 8\,kpc$, $R_s = 7\,kpc$,
a = – 13° is the pitch angle of the spiral arms and $\rho_0 = 30\times10^7$ for model A and $\rho_0 = 15\times10^7$ for model B (is the density of the spiral arms). Moreover,

$$K = \frac{2}{r|\sin(a)|},\quad D = \frac{1 + kh_z + 0.3(Kh_z)^2}{1 + 0.3\,Kh_z} \tag{8}$$

Considering a pattern speed Ω_{sp} of the spiral density wave, the Hamiltonian of the galactic model in the rotating frame of reference can be expressed as:

$$H = \frac{p_r^2}{2} + \frac{p_\varphi^2}{2r^2} - \Omega_{sp}\,p_\varphi + V_{ax}(r) + V_{sp}(r,\varphi) \tag{9}$$

where p_r is the radial velocity and p_φ is the angular momentum, in the inertial frame of reference, of the stars.

The families of stable periodic orbits, having shapes of precessing ellipses and supporting the spiral structure, can be found on the phase space of Hamiltonian (9) and are the continuation of the circular orbits of the axisymmetric part of the potential in the region of 2:1 resonance. Nevertheless, it is very difficult to locate these orbits in the normal phase spaces (r, p_r) or (φ, p_φ). So, we introduce action-angle variables (q, p) where q must be an angle (so the Ham-

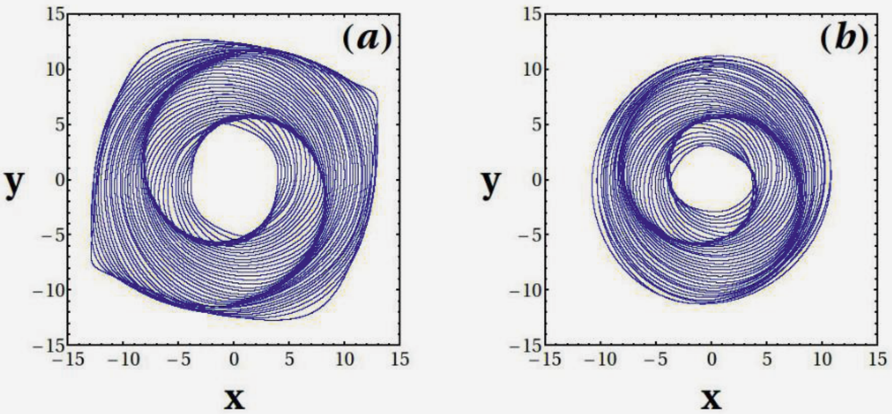

__Figure 3:__ Spiral density waves created by the x_1 family of elliptical orbits, found by the Poincare sections described in the text.
(a) Model (A) has a density $\rho_0 = 30\times10^7$ in equation (7). (b) Model (B) has a density $\rho_0 = 15\times10^7$ in equation (7). We observe that the density wave of the model (A) with the greater value of the perturbation is more intense and expands in larger distance from the center. Moreover, the elliptical orbits in model (A) have a more rectangular morphology near the end of the spiral arms. In both models the pattern speed of the density wave is $\Omega_{sp}= 20 km.sec^{-1}.kpc^{-1}$.

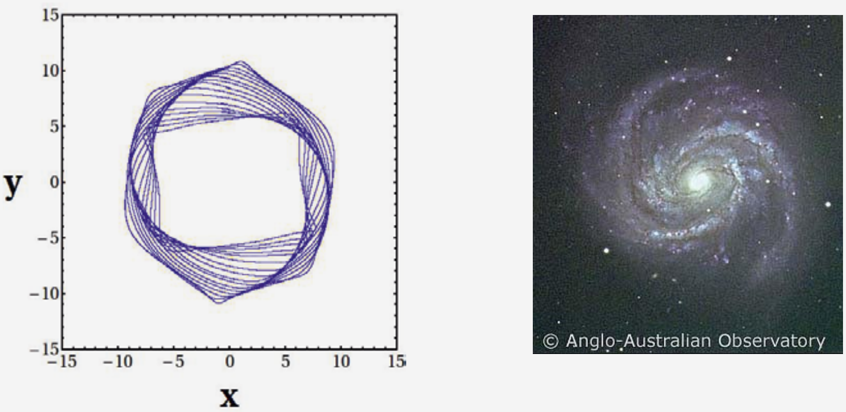

__Figure 4:__ On the left, model (C) with density $\rho_0 = 30\times10^7$ in equation (7). The pattern speed is $\Omega_{sp} = 30 km.sec^{-1}.kpc^{-1}$. The orbits of the x_1 family exist in a more limited area and create two pairs of spiral arms. On the right, the image of the grand design galaxy M100. This galaxy has clearly defined spiral arms and a well organised spiral structure. The precessing ellipses of Fig. 3 can well support the structure of such a galaxy.

iltonian should be periodic in q) and p is an action. According to this definition, the pair (φ, p_φ) is already an action-angle pair, while the pair (r, p_r) is not. We therefore introduce a new action-angle pair (θ_r, J_r), via the canonical transformation $(r, p_r) \rightarrow (\theta_r, J_r)$, related to the epicyclic oscillations:

$$(r - r_c) = \sqrt{\frac{2J_r}{k(r_c)}}\, sin(\theta_r) \qquad (10)$$

$$p_r = \sqrt{k(r_c)}\ \ J_r cos(\theta_r) \qquad (11)$$

where r_c is the radius of the circular orbit and

$$k(r_c) = \sqrt{\theta^2 V_0(r_c)/\theta r_c^2 + (3/r_c)(\theta V_0(r_c)/\theta r_c)}$$

is the corresponding epicyclic frequency.

Moreover, we introduce the "slow" angle $\psi = \theta r - 2\theta$, in order to locate the elliptical periodic orbits supporting the spirals, on the Poincaré section:

$$\xi = \sqrt{\frac{2J_r}{k(r_c)}} sin(\psi),\ \ p_\xi = \sqrt{2J_r k(r_c)} cos(\psi) \quad (12)$$

(see for details Efthymiopoulos, 2010).

These orbits belong to the x_1 family of orbits (see Contopoulos 1975).

In Figure 3, the precessing ellipses are plotted on the configuration space (x, y) for different values of the energy.

These ellipses are found from the Poincare section (ξ, p_ξ). For the model (A) (fig. 3a) the density is $\rho_0 = 30\times10^7$ and for the model (B) (fig. 3b) the density is $\rho_0 = 15\times10^7$ in equation (7). In both models the pattern speed of the spiral arms is $\Omega_{sp} = 20 km.sec^{-1} kpc^{-1}$. We observe that in model (A), which has the greater value of the perturbation's amplitude, the spiral density wave is more intense and expands in a larger distance from the center. Moreover, the elliptical orbits in model (A) have a more rectangular morphology near the end of the spiral arms, because they approach to the 4:1 resonance. The spiral arms end at this resonance (Contopoulos and Grosbol, 1986).

If we increase more the value of the perturbation's amplitude, chaos appears on the phase space and the regions of stable periodic orbits of the x_1 family are limited. Therefore, there is an upper limit of the amplitude of the spiral potential, above which no more regular elliptical orbits exist.

Then we increase the value of the pattern speed to $\Omega_{sp} = 30 km.sec^{-1} kpc^{-1}$ in model (C) (Left figure of Fig. 4).

The precessing ellipses of the x_1 family are limited in this case and two pairs of spiral arms appear.

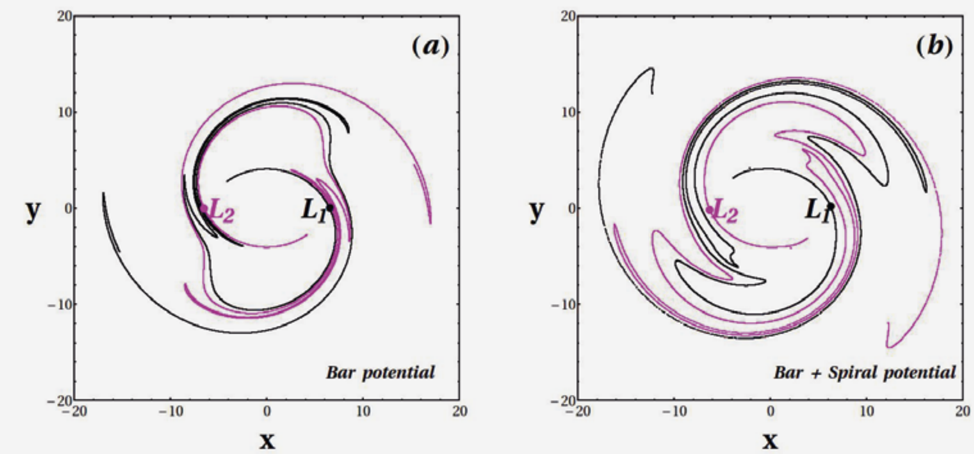

Figure 5: *(a) The apocentric manifolds that emanate from the unstable Lagrangian point L_1 (black curves) and from the unstable Lagrangian point L_2 (magenta curves) in the case of the bar bodel (16) and (b) in the case of the barred spiral model (17). The orbits are integrated for a small time interval.*

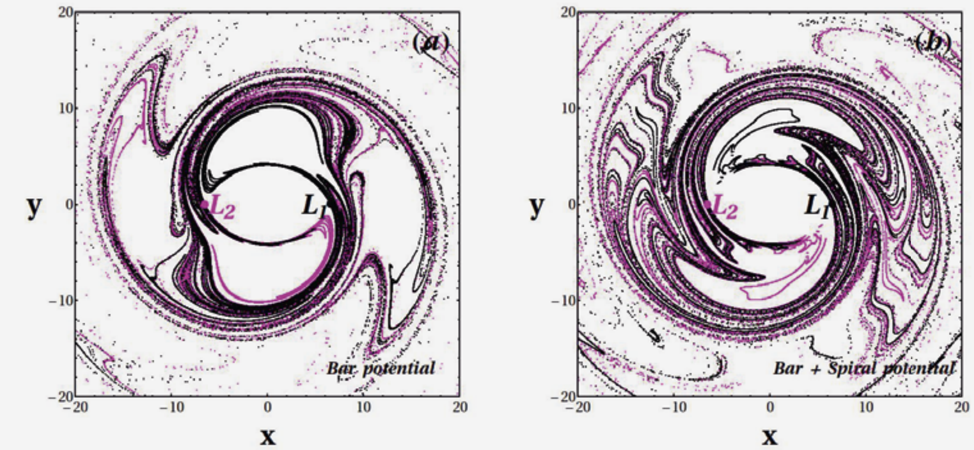

Figure 6: *The same with Fig. 5 but the orbits here are integrated for a much longer time. Spiral arms appear in the case of a barred galaxy (a) as well as in the case of a barred spiral galaxy (b). In (a) we observe also a ring perpendicular to the bar while in (b) there is no ring and the spiral arms emanate from the end of the bar.*

On the right of Fig. 4 we give the image of a grand design galaxy named M100. This galaxy has clearly defined spiral arms and a well organised spiral structure. The precessing ellipses of Fig. 3 can well support the structure of such a galaxy.

IV. Density waves in barred spiral galaxies

In the case where the spiral galaxy possess a bar (like in the case of the Milky Way galaxy) the density perturbation with respect to the axisymmetric background is so large that it can reach values greater than 50%. As a consequence, while the regular elliptical orbits can still support the bar structure, there exist no longer regular elliptical orbits outside the area of corotation that can support the spiral structure. Almost the whole percentage of the orbits outside corotation is chaotic. Therefore, in this case a new theory, called "manifold theory" can explain the way chaotic orbits can support the spiral structure.

In order to examine the "manifold theory", in the case of barred spiral galaxies we have used a model proposed by Pettitt et al. (2013) which simulates our own Milky Way galaxy (Efthymiopoulos et al., 2020). In reality we use the potential (1) introduced in the previous section and we add a potential for the bar:

$$V = V_{ax} + V_{bar} + V_{sp} \qquad (13)$$

The axisymmetric potential and the spiral potential are still given from relations (2)-(8) and we now add the potential of the bar given by Long and Murali (1992):

$$V_{bar} = \frac{GM_r}{2a} \ln\left(\frac{x - a + T_-}{x + a + T_+}\right) \qquad (14)$$

where $M_r = 6.25 \times 10^{10} M_\odot$ is the total mass of the bar and:

$$T \pm = \sqrt{(a \pm x)^2 + y^2 + b^2} \qquad (15)$$

with a and b the length of the semi-major and semi-minor axis respectively and $x = r\cos(\varphi)$, $y = r\sin(\varphi)$ are the cartesian coordinates of the orbits.

Considering a pattern speed of the bar Ω_{bar} the Hamiltonian of the bar model (without the spiral arms) in the rotating frame of the bar can be written (in polar coordinates) as:

$$H_{bar} = \frac{p_r^2}{2} + \frac{p_\varphi^2}{2r^2} - \Omega_{bar} p_\varphi + V_{ax}(r) + V_{bar}(r, \varphi) \qquad (16)$$

Figure 7: The image of a barred spiral galaxy named NGC 1365, one of the largest galaxies known to astronomers. Its spiral structure is supported by chaotic orbits as described in the text.

while the Hamiltonian of the barred spiral model, in the rotating frame of the bar (considering that the bar and the spiral arms have the same pattern speed Ω_{bar}), can be written (in polar coordinates) as:

$$H_{all} = \frac{p_r^2}{2} + \frac{p_\varphi^2}{2r^2} - \Omega_{bar} p_\varphi + V_{ax}(r) + V_{bar}(r,\varphi) + V_{sp}(r,\varphi) \quad (17)$$

A typical value of the pattern speed of the bar of the Milky Way, estimated by observations is $\Omega_{bar} = 40\, km.sec^{-1} \mathrm{kpc}^{-1}$ (see Gerhard, 2011).

The coordinates of the unstable equilibrium Lagrangian points L_1, L_2 of this galactic model can be found from the equation below:

$$\frac{dr}{dt} = \frac{dp_r}{dt} = \frac{d\varphi}{dt} = \frac{dp_\varphi}{dt} = 0 \quad (18)$$

The manifold theory that was introduced by Voglis et al., 2006, claims that the apocenters of the chaotic orbits with initial conditions on the unstable manifolds of the unstable Lagrangian points L_1, L_2 as well as of the unstable periodic orbits $P\,L_1$, $P\,L_2$ (which are the continuation of the unstable Lagrangian points in greater values of energies) support the spiral structure in the case of barred spiral galaxies. In a series of papers, after the introduction of the manifold theory, this theory have been studied and established in cases of galactic models as well as N-body simulations (Romero-Gomez et al. 2007, Tsoutsis et al. 2008, Tsoutsis et al. 2009, Athanassoula et al. 2009a,b, Romero-Gomez et al., 2011, Contopoulos and Harsoula 2012, Harsoula et al. 2016, Efthymiopoulos et al. 2019).

By studying the phase space (φ, p_φ) for $p_r = 0$ (apocenters) for the Hamiltonians (16) and (17) and for energies greater that the one corresponding to the Lagrangian points L_1 and L_2 ($H > H_{L1} = f(r_{L1}, p_{rL1}, \varphi_{L1}, p_{\varphi L1})$), we conclude that appart from the regular stable orbits around the Lagrangian equilibrium points L_4 and L_5, the rest of the phase space is totally chaotic. Moreover, N-body simulations have shown that particles avoid the area around L_4 and L_5, so statistically after corotation there are almost no regular orbits at all. We then locate the unstable periodic orbits PL_1 PL_2 (which are the continuation of L_1 L_2 for greater values of the energy H_{L1}) and we plot the corresponding apocentric manifolds. When we transport these apocentric manifols on the configuration space (x, y) we obtain the spiral morphology for the case of a barred galaxy (Fig. 5a) and for the case of a barred spiral galaxy (Fig. 5b). Black curves correspond to the to the apocentric manifolds emanating from the L_1 Lagrangian point (or the coresponding PL_1 orbit), while magenta curves correspond to the apocentric manifolds emanating from the L_2 Lagrangian point (or the coresponding PL_2 orbit). The orbits are integrated here only for a short time period. We observe that we can have well formed spiral arms even in the case of the barred model possessing no spiral arms (Fig. 5a). In this case a ring perpendicular to the bar is also created (a well know phenomenon in real galaxies). In the case of a barred spiral model (Fig. 5b) there is no ring but the spiral arms emanate directly from the end of the bar. Fig. 6 is the same as Fig. 5 but here the orbits are integrated for a much longer time interval. We see that the apocentric manifolds do not escape directly from the system but present a lot of recurrences and foldings before escaping from the galaxy and so they can support the spiral structure for long enough time comparing with the Hubble time.

Fig. 7 shows the image of a barred spiral galaxy named NGC 1365, one of the largest galaxies known. Astronomers think that the Milky Way may look very similar to this galaxy, but at half the size. Its spiral structure is supported by chaotic orbits through the manifold theory as described above.
In a recent paper, we have confirmed that the manifold theory still applies in the case where the bar has a different pattern speed than the spiral arms, which is a more realistic case for the barred spiral galaxies (Efthymiopoulos et al. 2020).

V. Discussion

There are two different Kinematic theories that can explain the creation of the spiral density waves of the galaxies in the case of grand design galaxies as well as in the case of barred spiral galaxies. The existence of regular elliptical orbits that support the spiral density waves in grand design galaxies depends on the amplitude of the perturbation as well as the pattern speed of the wave. The amplitude of the spiral perturbation cannot exceed a certain value because then chaos appears and regular elliptical orbits no longer exist. This fact may explain why the density perturbation of the grand design galaxies on the sky cannot exceed the value of approximately 10%-15% with respect to the axisymmetric background (see for example Elmegreen et al., 2011). Regarding the pattern speed of the spiral density wave, the values of

$$\Omega_{sp}=20\text{-}30 km.sec^{-1}kpc^{-1}$$

seems to be an upper limit for the existence of elliptical regular orbits that can support these spiral stuctures. This limit for the pattern speed of the spiral arms of grand design galaxies seems to be confirmed also by the observations of the real galaxies (see for example Sempere et al., 1995, Choi et al., 2015). On the other hand, the apocentric manifolds (consisting of chaotic orbits) can support the spiral structures in the case of barred spiral galaxies for long enough times and give a convincing alternative theory of the regular elliptical orbits.

References

1) C. Allen and A. Santillan, *Rev. Mex. Astron. Astrof.*, 22, 255 (1991)
2) Choi, Y. Dalcanton, J. J., Williams, B. F., Weisz, D. R., Skillman, E. D., Fouesneau, M., Dolphin, A. E., ApJ, 810, 9 (2015)
3) D. P. Cox and G. C. Gomez, *ApJS*, 142, 261 (2002)
4) A. Kalnajs, *Proc. Astron. Soc. Australia* 2, 174 (1973)
5) G. Contopoulos, *Astrophys. J.* 201, 566 (1975)
6) G. Contopoulos, P. Grosbol, *Astron. Astrophys.* 155, 11 (1986)
7) G. Contopoulos and M. Harsoula, *Cel. Mech. Dyn. Aston.*, 113,81, (2012).
8) C. Efthymiopoulos, *Eur. Phys. J. Special Topics* 186, 91 (2010)
9) C. Efthymiopoulos, P. Kyziropoulos, R. Paez, K. Zouloumi and G. Gravvanis, *MNRAS*, 484, 1487 (2019)
10) C. Efthymiopoulos, M. Harsoula and G. Contopoulos, *Astron. Astrophys*. 634, A44 (2020)
11) D. Elmegreen and 28 coauthors, *ApJ*, 737, 32 (2011)
12) O. Gerhard, *Mem. Soc. Astron. It. Supp.*, 18, 185, (2011).
13) M. Harsoula, C. Efthymiopoulos and G. Contopoulos, *Mon. Not. R. Astron. Soc.*, 459,3419, (2016)
14) C. Lin, F. Shu, *Astrophys. J.* 140, 646 (1964)
15) B. Lindblad, *Astrophys. J.* 92, 1 (1940)
16) B. Lindblad, Stockholm Obs. *Ann.* 21, 8 (1961)
17) K. Long, and C. Murali, 1992, *Astroph. J.*, 397, 44
18) M. Miyamoto and R. Nagai, *Astron. Soc. Jap. Pub.*, 27, 533 (1975)
19) P.A. Patsis, G. Contopoulos, P. Grosbol, *Astron. Astrophys.* 243, 373 (1991)
20) Pettitt A., Dobbs C., Acreman D., Price, D., *Mon. Not. R. Astron. Soc.*, 444, 919 (2013)
21) M. Romero-Gomez, J.J. Masdemont, E.M. Athanassoula, C. Garcia-Gomez, *Astron. Astrophys.*, 453, 39 (2006)
22) M. Romero-Gomez, M., E. Athanassoula, J. Masdemont and C. Garcia-Gomez, *Astron. Astroph.*, 472, 63 (2007)
23) E. Athanassoula, E., M. Romero-Gomez, M., J. Masdemont, *Mon. Not. R. Astron. Soc.*, 394, 67 (2009a)
24) E. Athanassoula, M. Romero-Gomez, A. Bosma, J. Masdemont, *Mon. Not. R. Astron. Soc*, 400, 1706 (2009b)
25) M. Romero-Gomez, E. Athanassoula, E., T Antoja, T. and F. Figueras, *Mon. Not. R. Astron. Soc.*, 418, 1176, (2011)
26) Sempere, M. J., Garcia-Burillo, S., Combes, F., Knapen, J. H., *Astron. and Astroph.*, 296, 45, (1995)
27) P. Tsoutsis, C. Efthymiopoulos and N. Voglis, *Mon. Not. R. Astron. Soc.*, 387, 1264 (2008)
28) P. Tsoutsis, C. Kalapotharakos, C. Efthymiopoulos and G. Contopoulos, *Astron. Astrophys.*, 495, 743, (2009)
30) N. Voglis, P. Tsoutsis, C. Efthymiopoulos, *Mon. Not. R. Astron. Soc.* 373, 280 (2006)

Linear and Circular polarization as a probe of physical conditions in AGN jets and outflows

by **Ioannis Myserlis**

Instituto de Radioastronomía Milimétrica, Avenida Divina Pastora 7, Local 20, E-18012 Granada, Spain, *e-mail: imyserlis@iram.es*

Max-Planck-Institut für Radioastronomie, Auf dem Hügel 69, D-53121 Bonn, Germany

Abstract:

As synchrotron sources, the radiation of jets and outflows emerging from active galactic nuclei (AGN) is both linearly and circularly polarized. Moreover, their intrinsic polarization can be further modified when the radiation propagates through magnetized plasma regions along the line of sight (e.g. through Faraday Rotation and Conversion). Consequently, though difficult to measure, linear and circular polarization can trace several physical conditions, such as the magnetic field strength and topology, the particle density and the plasma composition, both in the jet/outflow as well as along the line of sight. In the following, the physical conditions that can be investigated using linear and circular polarization is presented in a qualitative discussion. To facilitate such studies and reproduce the observed polarization, we have developed a full-Stokes (I, Q, U and V) radiative transfer model. Finally, an example study case is presented for the low-velocity outflow of the edge-on galaxy NGC 4845. Using a recent upgrade of our model, we managed to reproduce its polarization behavior and constrain physical conditions not only in the nuclear outflow but also its environment.

1. Introduction

Active galactic nuclei (AGN) can form jets and outflows that channel mass, momentum, energy and magnetic flux to the intergalactic medium (e.g. Blandford et al., 2019). Roughly 10% of AGN have highly collimated jets (Fig. 1, left) that move away from their central regions at relativistic velocities and can extend up to Mpc scales (e.g. Kellermann et al., 2016). However, lower velocity outflows (10^4–10^5 km/s) with wider opening angles (Fig. 1, right) are more frequently observed, in ~30%–40% of AGN (e.g. Tombesi et al., 2012). Both types of outflows emit synchrotron radiation and hence it is expected that they contain relativistic – or *mildly* relativistic – particles and magnetic fields.

Despite the fact that synchrotron radiation is intrinsically both linearly and circularly polarized (Sect. 2), the detection of polarized emission from AGN jets and outflows – especially in circular polarization – is very challenging due to the low polarization levels and possible depolarizing effects such as the complex source structure or a high level of disorder in the jets' magnetic fields. The net linear and circular polarization degree of AGN jets is on average ~3%–5% and ~0.5%, respectively, with the latter rarely reaching levels as high as 1%–2%, (e.g. Klein et al., 2003; Myserlis, 2015).

Nevertheless, linear and circular polarization measurements are extremely valuable in the investigation of physical conditions in AGN jets and outflows. The polarization parameters (linear and circular polarization degrees, circular polarization handedness and polarization angle) carry information about the physical conditions in the regions where the radiation is generated and through which it propagates, such as the magnetic field strength and topology, the particle density and the plasma composition, both in the jet/outflow as well as any magnetized plasma regions along the line of sight (Sects. 2,3)

This article presents a qualitative study of the physical conditions within the jet that can be inferred from linear and circular polarization measurements of AGN jets (Sects. 2,3). To facilitate such studies, we try to recreate the observed polarization using full-Stokes (*I, Q, U* and *V*) radiative transfer models, like the one presented in Sect. 4. Such models can account for the emission, absorption and propagation of the polarized radiation within the jets/outflows as well as in magnetized plasma regions along the line of sight. Finally, an example case for the low-velocity outflow of the edge-on galaxy NGC 4845 is presented in Sect. 5.

2. Synchrotron polarization

Synchrotron emission is intrinsically *elliptically* polarized, i.e. it has both linearly and circularly polarized components (e.g. Pacholczyk, 1970). As described below, the linear and circular polarization parameters depend on the physical conditions of the emitting medium, like its optical depth or plasma composition as well as the viewing angle.

Under the assumption that an ensemble of relativistic particles of a given type (e.g. e^- or e^+) are embedded in a uniform magnetic field B oriented at an angle θ with respect to our line of sight (Fig. 2, left), their energy distribution can be described by a power-law of the form:

$$N(E)dE = \kappa E^{-s} dE. \qquad (1)$$

These particles will emit synchrotron radiation with a convex spectral energy distribution (Fig. 2, right, top panel). The location of the spectral peak (both in frequency and intensity) depends on the particle density and the magnetic field strength in the emitting region. At frequencies higher than the peak, the volume of particles is optically thin and the spectrum is described by a power-law with index $a = -(s-1)/2$ that is typically measured to be -0.7. At frequencies lower than the peak, the emission is (self-)absorbed within the volume of emitting particles and its spectrum is described by a power-law of index +2.5. This is called the optically thick regime. The linear and circular polarization characteristics are very differ-

Figure 1: *Left: The highly collimated, relativistic jet emerging from the core of the elliptical galaxy Hercules A (Credit: NASA, ESA, S. Baum and C. O'Dea (RIT), R. Perley and W. Cotton (NRAO/AUI/NSF), and the Hubble Heritage Team (STScI/AURA)). Right: The low velocity outflow emerging from the nuclear region of the starburst galaxy M 82 (Credit: X-ray: NASA/CXC/JHU/D.Strickland; Optical: NASA/ESA/STScI/AURA/The Hubble Heritage Team; IR: NASA/JPL-Caltech/Univ. of AZ/C. Engelbracht)*

ent between the optically thick and thin regimes and provide additional information about the emitting region.

2.1. Intrinsic linear polarization

The linear polarization degree:

$$m_l = \sqrt{Q^2 + U^2}/I$$

in both spectral regions (optically thick and thin) depends on the index of the power-law energy distribution s in the following manner:

$$m_{l,\,\mathrm{thick}} = \frac{3}{6s + 13} \tag{2}$$

$$m_{l,\,\mathrm{thin}} = \frac{s+1}{s+7/3}\,. \tag{3}$$

For a typical value of s ~2.4 (a=0.7), $m_{l,\mathrm{thin}}$ ~72% and $m_{l,\mathrm{thick}}$ ~11% (Fig. 2, right, middle panel). Moreover, as shown in Fig. 2, there is a minimization (nulling) of m_l between the two spectral regions.

The net linear polarization of AGN jets and outflows, however, is usually much lower than the above theoretical values. For example, Fig. 3 shows the distribution of the average m_l for 73 AGN jets monitored over 4.5 years with the 100-m Effelsberg radio telescope at 8.35 GHz as part of the F-GAMMA monitoring program (Myserlis, 2015; Angelakis et al., 2017, 2019). The distribution has an average of 3.1%, i.e. much lower than the theoretical value. This discrepancy is usually attributed to a high level of disorder in the magnetic field or the complex source structure. In both cases, the integrated radiation can be considered as the superposition of N emitting regions with different magnetic field orientations and hence the net m_l drops as $1/\sqrt{N}$ from the theoretical value. This view is also supported by the fact that when the sources are resolved using high angular resolution observing techniques, such as Very Long Baseline Interferometry (VLBI), individual regions within the jet can have m_l much closer to the theoretical value (40-50%, e.g. Fig. 4).

Another difference between the two spectral regions is the polarization angle χ = 0.5 arctan(U/Q). In the opti-

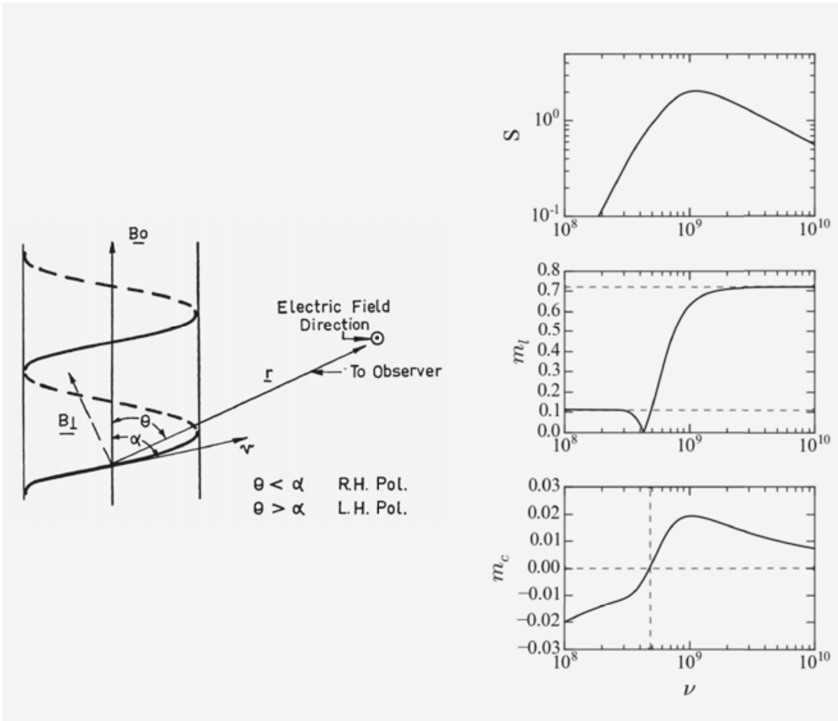

Figure 2: Left: *The spiral motion of a charged particle around a magnetic field line with pitch angle α. Figure taken from Gardner & Whiteoak (1966).* ***Right:*** *The frequency dependence of flux density S (top), linear polarization degree m_l (middle) and circular polarization degree m_c (bottom) for a synchrotron self-absorbed (SSA) source with a power-law energy distribution. m_l and m_c are normalized to 1.*

cally thin case, the polarization angle is oriented perpendicular to $B_\perp$, the magnetic field component on the plane of the sky (Fig. 2, left), whereas the optically thick polarization angle is parallel to that direction. As a result, when the opacity τ of a source with a given magnetic field configuration decreases (or increases), the angle can change by 90° as the medium becomes optically thin (or thick), *without* any change in the magnetic field (orientation). In conclusion, the intrinsic linear polarization can be used to trace $B_\perp$ and the optical depth τ of the emitting region.

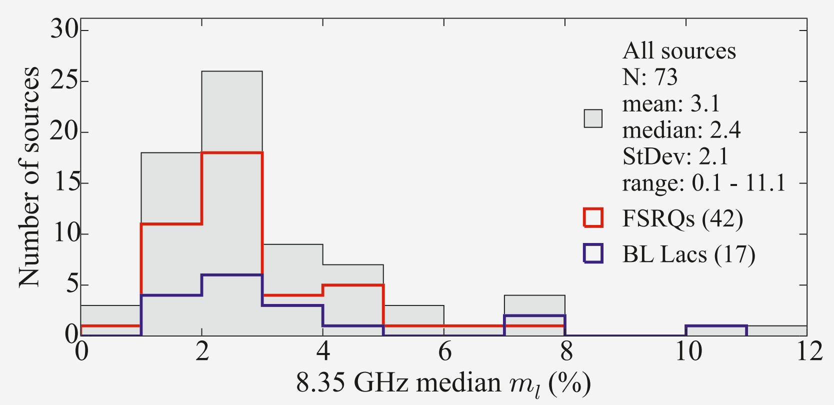

Figure 3: *The distribution of average m_l for 73 AGN jets that were monitored over 4.5 years with the 100-m Effelsberg radio telescope at 8.35 GHz, as part of the F-GAMMA program.*

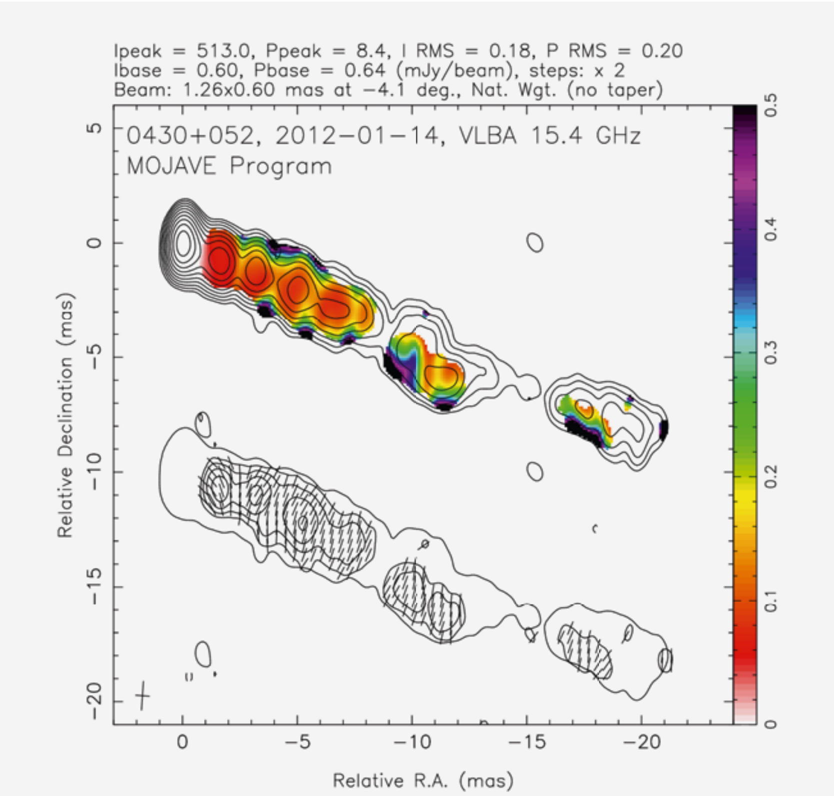

Figure 4: *The relativistic jet of the blazar 3C 120, observed with the Very Long Baseline Array (VLBA) at 15.4 GHz, as part of the MOJAVE monitoring program (Lister et al., 2018). In the top, the total flux density (Stokes I) contours are overlaid with the linear polarization degree m_l according to the color bar on the right. In the bottom, the linearly polarized flux density $\left(\sqrt{Q^2+U^2}\right)$ is shown with contours and the short bars indicate the polarization angle orientation. The lowest Stokes I contour appears around the bottom image to show registration.*

2.2. Intrinsic circular polarization

As mentioned above, synchrotron radiation is elliptically polarized, which means that it has also an intrinsic circularly polarized component (Stokes V).

For a single charged particle gyrating around a magnetic field line, the handedness of its circular polarization depends on the angle $\psi = \theta - a$, where θ is the angle between the magnetic field and the line of sight and a is the angle between the magnetic field and the velocity vector of the gyrating particle, or its pitch angle (Fig. 2, left).

For high energy particles (large Lorentz factor γ), Stokes V contains only odd terms in ψ, being positive (right-handed) when $\psi < 0$ and negative (left-handed) when $\psi > 0$ (in the case of e^-). Therefore, for an ensemble of high energy particles with an isotropic pitch angle distribution (equal number of positive and negative ψ), the net circular polarization is zero. However, for mildly relativistic plasmas (lower γ), Stokes V has both odd and even terms of ψ, and hence the net circular polarization is small but nonzero, even for an isotropic pitch angle distribution.

Furthermore, there is an inherent pitch angle (and therefore ψ) anisotropy for any non-uniform particle energy distribution, like the power-law assumed in Eq. 1. The critical frequency of synchrotron emission, at which most energy is radiated, is:

$$\nu_c \propto \gamma^{-2} \omega_g \sin a \qquad (4)$$

where ω_g is the gyrofrequency of the emitting particles. Therefore, for a steep energy (or γ, since $E = \gamma mc^2$) distribution, we observe more particles with smaller a at the critical frequency. This introduces a pitch angle anisotropy, giving rise to a net circular polarization. The net circular polarization degree for an ensemble of particles is of the order of γ^{-1} and it has a frequency dependence of $\nu^{-0.5}$ (Fig. 2, right, bottom panel). Finally, the Stokes V sign (handedness) depends on the orientation of $B_{||}$, the magnetic field component along the line of sight (which is equivalent to the dependence on ψ described above) as well as the charge sign of the emitting particles. Moreover, as shown in Fig. 2 (right, bottom panel), there is a smooth sign change of $m_c = V/I$, going through a minimization (nulling) between the two spectral regions (optically thick and thin). In conclusion, the intrinsic circular polarization can be used to trace $B_{||}$, the pitch angle distribution, the charge sign and the optical depth τ of the emitting region.

It is important to to note that the polarization characteristics discussed above are computed in the rest frame of the emitting plasma. When analyzing polarimetric observations, especially in the case of AGN jets, we need to take into account the relativistic motion of the emitting region. For example, when we use the polarization angle to trace the magnetic field orientation, we need to consider that it can be significantly modified due to relativistic aberration (e.g. Blandford & Königl, 1979).

3. Polarization propagation effects

The intrinsic polarization parameters described in Sect. 2 can be modified when the radiation propagates through magnetized plasma regions along the line of sight. The two main polarization propagation effects are Faraday Rotation and Conversion.

3.1. Faraday Rotation

Faraday Rotation is a birefringent effect that occurs when linearly polarized radiation is propagated through a magnetized plasma region. The effect is maximized when the region contains low-energy plasma and its magnetic field is parallel to the line of sight. In this case, the propagation modes are circularly polarized. Therefore, when a linearly polarized wave propagates through the region, its two circularly polarized components are traveling with different velocities, introducing a phase difference between them. This phase difference is manifested as a wavelength-dependent rotation of the polarization angle

$$\Delta_X = \left[\frac{e^3}{2\pi m^2 c^4}\int_0^d n_e(s)\, B_{\|}(s)\, ds\right]\lambda^2 \qquad (5)$$
$$= RM\lambda^2$$

where d is the size of the magnetized plasma region, n_e is its particle density and $B_{||}$ is the magnetic field strength along the line of sight. The quantity in square brackets in Eq. 5 is called rotation measure (RM) and its sign depends on the direction of $B_{||}$ along the line of sight.

Faraday Rotation can potentially decrease the amount of linear polarization of the emitting region if (a) the energy distribution extends to (very) low γ_{min} values or (b) it contains a significant amount of cold plasma. In that case, the radiation generated at various depths within the emitting region undergoes different amounts of rotation, thus decreasing the net linear polarization degree of the emerging radiation (depolarizaton). This variant of the effect is often referred to as *internal* Faraday Rotation. In conclusion, Faraday Rotation can be used to trace $B_{||}$ (both strength and direction) and the density of low-energy particles (n_e) in magnetized plasma regions between the source and the observer (e.g. Burn, 1966; Pacholczyk, 1977; Wardle & Homan, 2003)

3.2. Faraday Conversion/Pulsation

Faraday Conversion is another birefringent effect that occurs when polarized radiation is propagated through a magnetized plasma region. The effect is maximized when the region contains (mildly) relativistic plasma and its magnetic field is perpendicular to the line of sight. In this case, the propagation modes are linearly polarized (or highly elliptical) and perpendicular to each other, with the ordinary one being parallel to the magnetic field of the region. Therefore, when a polarized wave (linearly or circularly) propagates through the region, its two linearly polarized components are traveling with different velocities, introducing a phase difference between them. This phase difference is manifested as a (partial) inter-conversion between linear and circular polarization, keeping the total polarization degree constant. As the radiation propagates, Stokes U and V change in a cyclic pattern: $U \rightarrow V \rightarrow -U \rightarrow -V \rightarrow U \rightarrow V \ldots$ Therefore, the effect has also been called Faraday Pulsation (e.g. Pacholczyk, 1977).

Faraday Conversion is maximized when there is a 45° difference between the polarization angle of the incident radiation and the magnetic field direction of the intervening plasma region. Therefore, Faraday Conversion is very low in a synchrotron emitting region since its linear polarization is either perpendicular or parallel to the magnetic field direction in the optically thin and thick regime, respectively. Nevertheless, the misalignment of the polarization angle needed for Faraday Conversion can arise from (a) internal Faraday Rotation, (b) a random magnetic field component in the emitting region or (c) a large scale ordered magnetic field with different orientations between the front and the back side of the region, e.g. following a helical pattern (e.g. Enßlin, 2003). Finally, Faraday Conversion shows also a frequency dependence that is generally more steep than the intrinsic circular polarization with indices between −1 and −5 (Wardle & Homan, 2003). In conclusion, Faraday Conversion can be used to trace $B_\perp$ and the density of (mildly) relativistic magnetized plasma between the emitting source and the observer.

As shown by the above discussion, we can probe several physical conditions in the regions where synchrotron radiation is emitted and propagates using polarization observations. If possible, it is essential to measure both linear and circular polarization *simultaneously* because they provide complementary information (e.g. $B_\perp$ and $B_{||}$) and hence we need both to draw the full picture.

4. Polarized radiative transfer model

In order to study the polarization characteristics of AGN jets and outflows systematically and use them to constrain the physical conditions described in Sects. 2 and 3, we have developed a polarized radiative transfer model. The model emulates the emission of astrophysical plasma systems in all four Stokes parameters *I, Q, U,* and *V*, accounting also for propagation effects, such as Faraday Rotation and Conversion.

In particular, we model an AGN outflow as an ensemble of cells organized in a three-dimensional shape (e.g. paraboloid or conical). Each cell contains homogeneous relativistic plasma with a power-law energy distribution and a uniform magnetic field (Fig. 5). The emission of the modeled jet is calculated by solving the full-Stokes radiative transfer problem for radiation emitted and propagated across the jet using the equations given in Jones & Odell (1977) and Hughes et al. (1989). Finally, we sum the Stokes parameters *I, Q, U* and *V* emerging from each slab and use this result to calculate the net

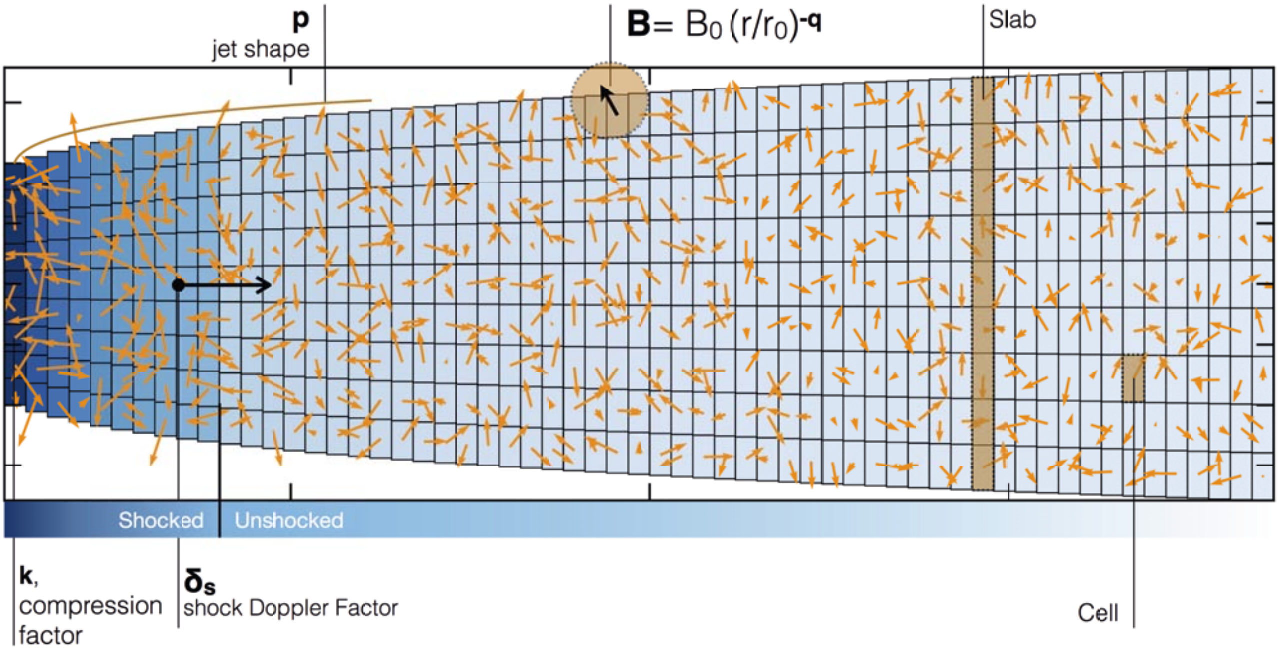

Figure 5: *A model jet profile and some key parameters of the radiative transfer code. The density gradient along the jet axis is highlighted by the color shading of the cells. The orange arrows show the projection of magnetic field on the plane of the sky.*

linear and circular polarization of the modeled jet/outflow. Given the low values of polarization degree that are usually observed, the model assumes a predominantly turbulent magnetic field configuration, as shown in Fig. 5.
The model contains also a physical mechanism to change the conditions in the simulated jet. Variability is induced via the downstream propagation of relativistic shock fronts which modify the local physical conditions (plasma density, magnetic field strength and topology, as well as particle energy distribution power-law index). These changes are imprinted on the emitted spectrum which follows the shock evolution (e.g. Marscher & Gear, 1985). A more detailed description of the model can be found in Myserlis (2015); Myserlis et al. (2016).

The radiative transfer model has been successfully tested from low- to high-energy plasma flows, where the Faraday effects become progressively suppressed. In the high-energy plasma case of the blazar 3C 454.3 (Myserlis et al., 2016), we reproduced the temporal evolution of all four Stokes parameters observed during a flaring event between MJD 55400 and 56500. The physical conditions that were constrained are the coherence length of the magnetic field (~ 9 pc), the shock compression factor (k ~ 0.8) as well as

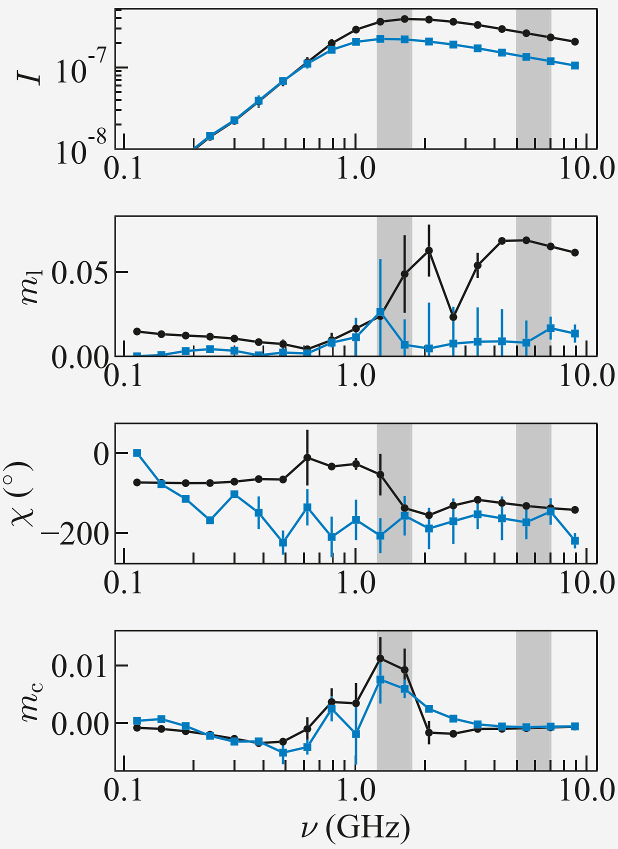

Figure 6: *From top to bottom: The frequency dependence of Stokes I, linear polarization degree m_l, polarization angle χ and circular polarization degree m_c, as produced by our radiative transfer code to model the polarization behavior of the nuclear outflow in NGC 4845. m_l and m_c are normalized to 1. The black circles and blue squares correspond to model realizations without and with a cold plasma "screen" around the outflow, respectively. The suppression of m_l at 6 GHz with the cold plasma "screen" is clearly evident. See text for more details.*

its Doppler factor ($D \sim 30$). The low-energy plasma case of NGC 4845 (Angelakis et al., 2017), along with a recent revision of the model, is presented in more detail in the following section.

5. The case of NGC 4845

As a study of low-energy plasma, where the Faraday effects are expected to be enhanced, we focused on the linear and circular polarization of the nuclear outflow observed in the edge-on galaxy NGC 4845 (Irwin et al., 2015). Irwin et al. (2015) observed the source using the Karl G. Jansky Very Large Array (VLA) at two bands, 1.5 GHz and 6 GHz (shaded frequency ranges in Fig. 6). Their findings suggest that the source has a synchrotron self-absorbed (SSA) spectrum with a peak at ~1.8 GHz, its linear polarization degree is very low in both bands (0.1%-0.5%) but – interestingly – its circular polarization degree is extremely high at 1.5 GHz (~2%-3%) and zero at 6 GHz. As presented in Angelakis et al. (2017), we were able to reproduce most of the observed polarization parameters by using our model to create a conical, adiabatically expanding outflow with a predominantly turbulent magnetic field configuration and significant population of low-energy particles ($\gamma_{min} \sim 10$-100). The low-energy plasma enhances the Faraday effects at 1.5 GHz reducing the net linear polarization, due to internal Faraday Rotation, and increasing the net circular polarization as a result of Faraday Conversion (Fig. 6, black circles).

However, as shown in Fig. 6 (black circles), this model can not explain the low linear polarization degree at 6 GHz. It was speculated that this behavior could be explained by "an excess of low-energy magnetized plasma within or around the flow may be causing depolarization through Faraday rotation" (Angelakis et al., 2017). To test for this effect, we upgraded our model to include an excess component of cold plasma. Cold plasma does not have a strong effect on the emission or absorption of synchrotron radiation, but it can have a significant contribution to the transformation of polarization (Faraday Rotation or Conversion). The propagation coefficients that we implemented are given in Jones & Odell (1977) (Eq. C12).

As a result, the observations could be easily reproduced by propagating the emerging radiation through a cold plasma "screen" of size equal to the modeled outflow or larger. The suppression of linear polarization at 6 GHz can be achieved when the cold plasma density in the screen is at least ~40-50% of the plasma density in the outflow (Fig. 6, blue squares). As discussed in (Irwin et al., 2015), this screen could be a dynamic sheath of cold gas entrained with the nuclear outflow or a stationary surrounding cloud.

6. Summary & Conclusions

Linear and circular polarimetry are extremely valuable tools in the study of AGN jets and outflows. Though difficult to measure, the linear and circular polarization parameters can be used to trace several physical conditions, such as the magnetic field strength and topology, the particle density and the plasma composition, both in the jet/outflow as well as any magnetized plasma regions along the line of sight (Sects. 2 and 3).

To study the polarization of AGN jets and outflows systematically and constrain their physical conditions, we developed a polarized radiative transfer model that accounts for the emission, absorption, and propagation of synchrotron radiation (Sects. 4). As an example study of low-energy plasma, we modeled the linear and circular polarization observed at the center of the edge-on galaxy NGC 4845 as a conical, adiabatically expanding outflow with a predominantly turbulent magnetic field configuration and significant population of low-energy particles ($\gamma_{min} \sim 10$-100). To reproduce the observed behavior accurately, we recently upgraded the model and implemented a "screen" of cold plasma around the modeled outflow that suppresses the linear polarization degree as a result of Faraday Rotation.

References

Blandford, R., Meier, D., & Readhead, A. 2019, ARA&A, 57, 467

Kellermann, K. I., Condon, J. J., Kimball, A. E., et al. 2016, ApJ, 831, 168

Tombesi, F., Cappi, M., Reeves, J. N., et al. 2012, MNRAS, 422, L1

Myserlis, I. 2015, Ph.D. Thesis, Max-Planck-Institut für Radioastronomie, http://kups.ub.uni-koeln. de/6967/

Klein, U., Mack, K.-H., Gregorini, L., et al. 2003, A&A, 406, 579

Pacholczyk, A. G. 1970, Radio Astrophysics, Series of Books in Astronomy and Astrophysics

Gardner, F. F., & Whiteoak, J. B. 1966, ARA&A, 4, 245

Angelakis, E., Myserlis, I., & Zensus, J. A. 2017, Galaxies, 5, 81

Angelakis, E., Fuhrmann, L., Myserlis, I., et al. 2019, A&A, 626, A60

Lister, M. L., Aller, M. F., Aller, H. D., et al. 2018, ApJS, 234, 12

Blandford, R. D., & Königl, A. 1979, ApJ, 232, 34

Burn, B. J. 1966, MNRAS, 133, 67

Pacholczyk, A. G. 1977, Radio Galaxies, Oxford Pergamon Press International Series on Natural Philosophy, 89

Wardle, J. F. C., & Homan, D. C. 2003, Ap&SS, 288, 143

Enßlin, T. A. 2003, A&A, 401, 499

Jones, T. W., & Odell, S. L. 1977, ApJ, 214, 522

Hughes, P. A., Aller, H. D., & Aller, M. F. 1989, ApJ, 341, 54

Marscher, A. P., & Gear, W. K. 1985, ApJ, 298, 114

Myserlis, I., Angelakis, E., Kraus, A., et al. 2016, Galaxies, 4, 58

Irwin, J. A., Henriksen, R. N., Krause, M., et al. 2015, ApJ, 809, 172

Solar Orbiter: Europe's new mission to the Sun

by **Yannis Zouganelis**
European Space Agency

1. Introduction

More than four centuries have passed since the first observation of sunspots with a telescope and more than six decades since the discovery of the solar wind. Yet the fundamental mysteries of our star and of its extended atmosphere remain unsolved, with each new observation revealing complex physical phenomena that we strive to understand from inside the Sun's sphere of influence, the heliosphere. Understanding the physics and the coupling between the Sun and the heliosphere is the main goal of Solar Orbiter, a space mission of international collaboration between ESA and NASA. Launched on 10 February 2020, the Solar Orbiter spacecraft will study the Sun and the inner heliosphere with a unique combination of six remote-sensing instruments observing the Sun and solar corona, and four in-situ instruments measuring the properties of the solar plasma around the spacecraft. Together, the ten Solar Orbiter instruments will provide a complete description of the plasma making up the solar wind – its origin, transport and composition – vastly improving on the earlier Helios missions[1], launched in 1974 and 1976, and complementing the new measurements of NASA's Parker Solar Probe mission[2].

Figure 1: *Artist's impression of Solar Orbiter. Credit: ESA/ATG Medialab.*

2. Science goals and mission profile

Solar Orbiter is the first medium-class mission of ESA's "Cosmic Vision" programme, developed by scientists and engineers from almost all European countries, and implemented together with NASA. It builds on the success of previous collaboration between ESA and NASA on two major solar missions (see Fig. 2 for the whole list of solar missions since 1990): SOHO (launched in 1995), a mainly remote-sensing mission, and Ulysses (1990-2009), an in-situ probe that was the first spacecraft to leave the plane of the ecliptic. Both have revolutionised the way we think of the Sun and the heliosphere. Solar Orbiter is the conceptual combination of these two missions – an out-of-ecliptic in-situ exploratory probe bringing state-of-the-art telescopes closer to the Sun than ever before. In addition, joint observations with NASA's Parker Solar Probe, which approaches so close to the Sun that it could not carry telescopes to observe the solar disk, will deliver new and potentially disruptive results.

The supersonic solar wind, driven by dynamic plasma and magnetic processes at the Sun's surface, expands to surround the planets of our solar system, as well as the space far beyond them. In the solar interior, the solar dynamo drives magnetic fields whose buoyancy brings them to the surface where they form huge arcades of loops, which store enormous amounts of magnetic energy. These magnetic loops are stretched and sheared by the Sun's differential rotation and transient surface processes, eventually erupting in bright explosions, which eject magnetic structures and accelerate energetic particles that fly into the solar system, occasionally impacting Earth and its magnetic shield with disruptive effects on space and terrestrial systems. Understanding the complex physical processes at work in this system is the central goal of heliophysics. Since the Sun and presumably the heliosphere are typical of many late-type main-sequence stars and their astrospheres, these studies are relevant to astrophysics, but are unique since the Sun alone is close enough for detailed study.

Although Earth's vantage point at 1 au is close by astrophysical measures, it has long been known that much of the crucial physics in the formation and activity of the heliosphere takes place much closer to the Sun, and that by the time magnetic structures, shocks, energetic particles and the solar wind pass by Earth, they have already evolved and in many cases mixed, blurring the signatures of their origin. With the prov-

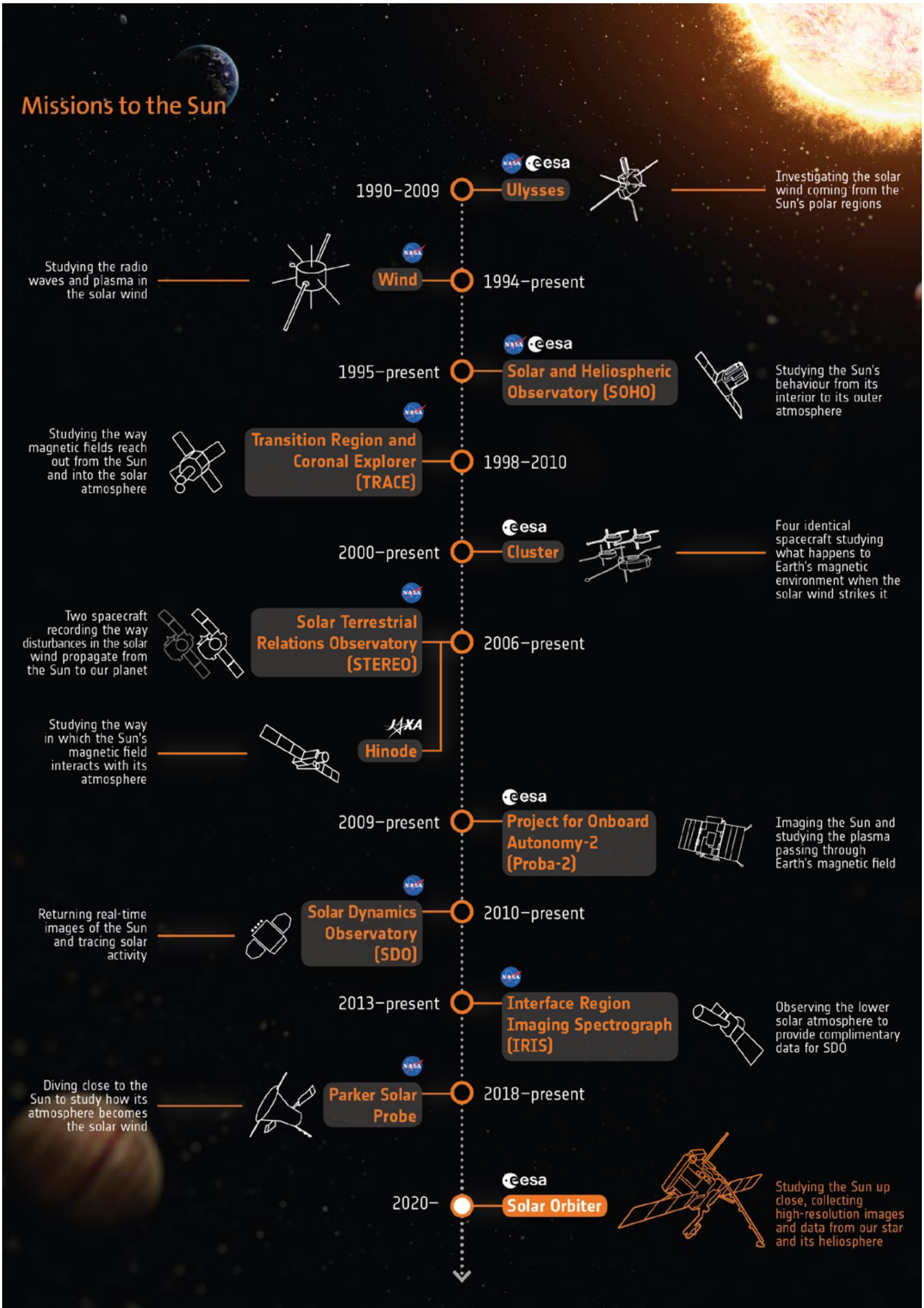

***Figure 2:** Solar missions since 1990. Credit: ESA.*

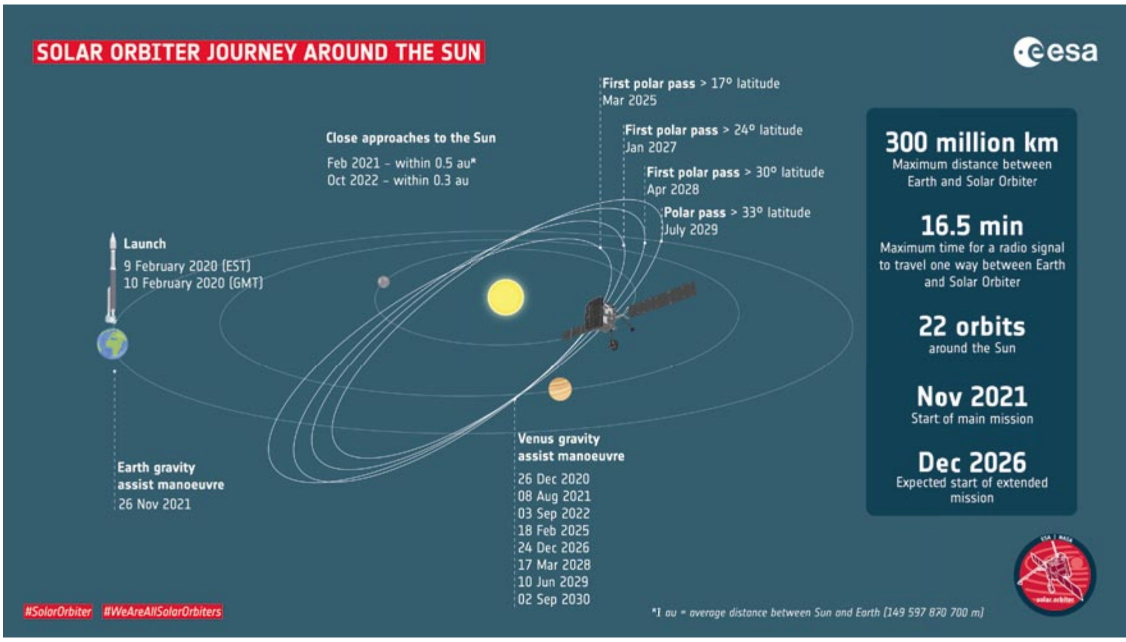

Figure 3: *Solar Orbiter orbits and mission timeline. Credit: ESA*

en effectiveness of combined remote and in-situ studies, critical new advances are expected to be achieved by Solar Orbiter that takes this principle much closer to the Sun.

With Solar Orbiter's unique combination of close distance to the Sun (minimum perihelion of 0.28 au), and out-of-ecliptic vantage points (reaching over 33° of heliographic latitude), the sources on the surface of the Sun will be identified and studied accurately and combined with in-situ observations of solar wind, shocks, energetic particles, etc., before they have a chance to evolve significantly. Moreover, the highly inclined orbit will allow a first-ever look at the solar poles, crucial to understand the solar interior and solar activity.

The design of the mission has been driven by the need to answer the following four interrelated top-level questions[3]:

– What drives the solar wind and where does the coronal magnetic field originate?
– How do solar transients drive heliospheric variability?
– How do solar eruptions produce energetic particle radiation that fills the heliosphere?
– How does the solar dynamo work and drive connections between the Sun and the heliosphere?

3. Payload

To answer these challenging questions, it is essential to make in-situ measurements of the solar wind plasma, fields, waves, and energetic particles close enough to the Sun that they are still relatively pristine and have not had their properties modified by subsequent transport and propagation processes. This is one of the fundamental drivers for the Solar Orbiter mission and its unique trajectory. It will measure the solar wind and at the same time try to identify, using its comprehensive telescopes package, the sources of the plasma when it left the Sun. The in-situ instruments comprise a Solar Wind Analyser (SWA; for measuring the properties of electrons, protons and heavy ions), a Magnetometer (MAG), a Radio and Plasma Waves (RPW) experiment and the Energetic Particle Detector (EPD) suite. The remote-sensing payload consists of an extreme UV full-Sun and high-resolution imager (EUI), a coronagraph (Metis), a Polarimetric and Helioseismic Imager (PHI), a heliospheric Imager (SoloHI), an extreme UV spectral imager (SPICE), and an X-ray telescope and spectrometer (STIX). In the following sections, we briefly describe the overarching goal of each instrument. A more detailed description can be found in the mission and instrument papers published in the 2020 special issue of A&A[*] on Solar Orbiter.

* https://www.aanda.org/component/toc/?task=topic&id=1082

3.1. The in-situ instruments

EPD, the Energetic Particle Detector, will measure the energetic particles that flow past the spacecraft. It will look at their composition and variation over time. The data will help investigate the sources, acceleration mechanisms, and transport processes of these particles.

The Magnetometer MAG has two elements that will measure the magnetic field around the spacecraft with high precision. It will help determine how the Sun's magnetic field links to the rest of the Solar System and changes with time. This will help us understand how the corona is heated and how energy is transported in the solar wind.

The Radio and Plasma Waves (RPW) instrument will measure the variation of magnetic and electric fields using a number of sensors and antennas. This will help to determine the characteristics of waves and fields in the solar wind. RPW is the only instrument on Solar Orbiter that makes both in-situ and remote-sensing measurements.

The Solar Wind Analyser (SWA) consists of a suite of sensors that will measure the solar wind's bulk properties, such as density, velocity and temperature. It will also measure the composition of the solar wind. This will be done for the first time in the inner heliosphere.

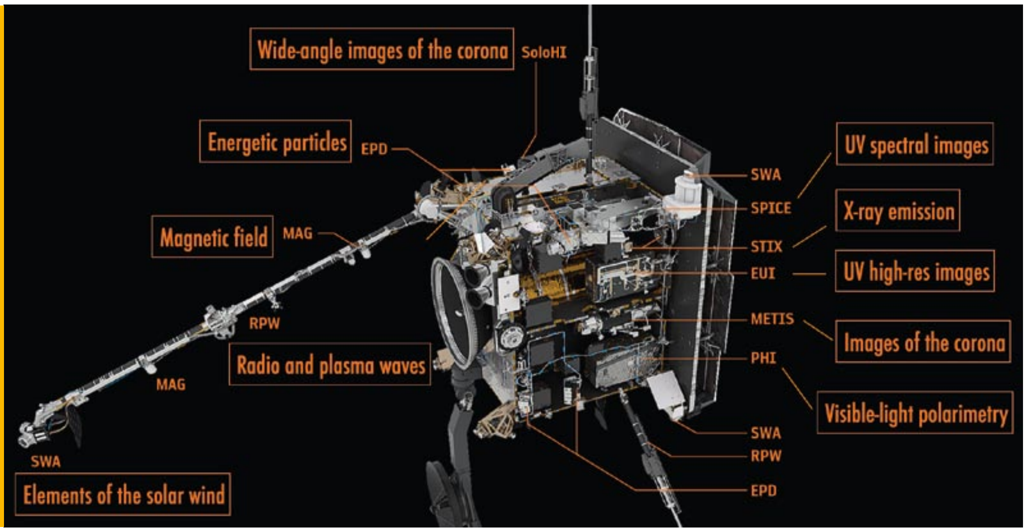

Figure 4: *Solar Orbiter spacecraft backside and payload. Credit: ESA*

3.2. The remote-sensing instruments

The Extreme Ultraviolet Imager (EUI) will take images of the solar chromosphere, transition region and corona. This will allow us to investigate the mysterious heating processes that take effect in this region and will enable in-situ measurements of the solar wind to be related back to their source regions on the Sun.

The Metis coronagraph will take simultaneous images of the corona in visible and ultraviolet wavelengths. This will reveal the structure and dynamics of the solar atmosphere in unprecedented detail, stretching out from 1.7 to 4.1 solar radii and offer us the opportunity to look for the link between the behaviour of these regions and space weather in the inner solar system.

The Polarimetric and Helioseismic Imager (PHI) will provide high-resolution measurements of the magnetic field across the photosphere, and maps of its brightness at visible wavelengths. It will also produce velocity maps of the movement of the photosphere that will allow helioseismic investigations of the solar interior, in particular the convective zone.

The Heliospheric Imager SoloHI will take images of the solar wind by capturing the light scattered by electron particles in the wind. This will allow the identification of transient disturbances in the solar wind, such as the type triggered by a coronal mass ejection, in which a billion tonnes of coronal gas can be ejected outwards into space.

The SPICE spectroimager (Spectral Imaging of the Coronal Environment) will reveal the properties of the solar transition region and corona by measuring the extreme ultraviolet wavelengths given off by the plasma. This data will be matched to the solar wind properties that are subsequently detected by the spacecraft's in-situ instruments.

The STIX X-ray Spectrometer/Telescope will detect X-ray emission coming from the Sun. This could originate from hot plasma, often related to explosive magnetic activity such as solar flares. STIX will record the timing, location, intensity, and energy data for these events so that their effects on the solar wind can be better understood.

4. Technological Challenges

Solar Orbiter must operate for years in one of the most hostile regions of the solar system. At closest approach, approximately 42 million kilometres from the Sun, it will be at just over a quarter of the distance between the star and our planet. Not even the scorched inner planet Mercury gets this close to the Sun. The closest Mercury ever approaches is around 46 million kilometres, but that's still enough to heat its surface to around 430°C – more than hot enough to melt lead.

To protect the 1.8 tonne spacecraft from such extremely high temperatures, ESA and the spacecraft's prime contractor, Airbus Defence and Space, have developed unique heatshield technologies with other industrial partners. In particular, the Irish company Enbio has developed a novel product called SolarBlack. SolarBlack is a calcium phosphate preparation that has been applied to the outermost layer of Solar Orbiter's heatshield (see Fig. 5). It is excellent at absorbing heat and will not decay by shedding layers, or gradually turn into gas, no matter how much infrared and ultraviolet radiation it absorbs. Behind this thin layer of SolarBlack, the outer portion of the heatshield is made up of twenty wafer-thin layers of titanium, which can withstand temperatures of up to 500°C. Behind this is a gap, which guides the heat out to the sides and away from the spacecraft. The only bits of hardware that cross this gap are ten star-shaped brackets that attach the top layer of the heatshield to the base. The base itself is a 5 cm-thick aluminium honeycomb that is covered by 30 layers of lower-temperature insulation. This can handle temperatures of up to 300°C. The entire heatshield is then fixed to the spacecraft by ten 1.5 mm-thin titanium 'blades' to minimise the transfer of heat through the spacecraft's superstructure.

The heatshield is the critical technological component which makes this mission possible, as Solar Orbiter will be subjected to thirteen times the amount of solar heating that satellites in Earth's orbit experience. However, the remote-sensing instruments still have to look towards the Sun in order to make observations. Small sliding doors in the heatshield (Fig. 5) let sunlight into the internally-mounted remote-sensing instruments. On most of these, special windows block out most of the heat to protect the in-

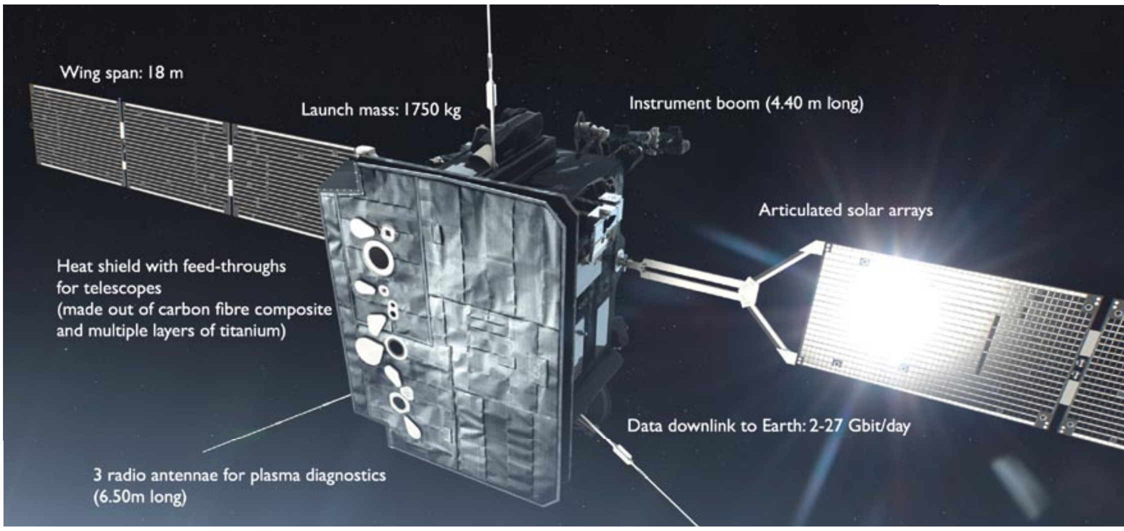

Figure 5: *Solar Orbiter spacecraft frontside. Credit: ESA*

strument, though two have other arrangements: the SPICE instrument allows all the light in and internally filters out what it doesn't want, and the wide-field camera, SoloHI, peeks around the side of the sunshield but doesn't look at the Sun directly. The in-situ instruments measure the conditions around the spacecraft itself. Some can remain in the shadow of the heatshield; others must look towards the Sun and so are equipped with their own mini heat-shields or protection.

Solar Orbiter relies on solar power to generate its electricity. It consists of solar panels that can be rotated, so that when the spacecraft is close to the Sun the panels can be angled away to protect them from getting too hot. When Solar Orbiter is in the outer parts of its orbit, however, the arrays can be rotated face-on to provide enough power (see Fig. 5).

5. Summary

The Solar Orbiter spacecraft launched on 10 February 2020 (05:27 CET) on an Atlas V 411 launcher from Cape Canaveral. After a short commissioning phase, the in-situ payload will be fully operational as of mid-June 2020, during Solar Orbiter's first perihelion at 0.51 au. The nominal phase, with all 10 instruments operating, will start in November 2021 and run until the end of 2025, with possible extensions up to 2030. Following the open-data philosophy of most solar missions, all science data will be publicly available three months after their reception on the ground, a period needed for calibration and checking. The international solar and heliophysics community is now ready for an exciting and busy decade, which will certainly transform our knowledge of the Sun.

References

1. Schwenn, R. & Marsch, E. *Physics and Chemistry in Space, Vol. 20, Physics of the Inner Heliosphere I. Large-Scale Phenomena,* ed. R. Schwenn & E. Marsch (Berlin: Springer-Verlag) (1990).
2. Fox, N. J. *Space Sci. Rev.* **204**, 7–48 (2016).
3. Müller, D., Marsden, R. G., St. Cyr, O. C. & Gilbert, H. R. *Sol. Phys.* **285**, 25–70 (2013).

Visit our website

http://www.helas.gr

The above web server contains information, both in greek and english, about the Hellenic Astronomical Society (Hel.A.S.), the major organization of professional astronomers in Greece. The Society was established in 1993, it has more than 250 members, and it follows the usual structure of most modern scientific societies. The web pages provide information and pointers to astronomy related material, useful to both professional and amateur astronomers in Greece. It contains a directory of all members of the Society, as well as an archive of all material published by the Society, including electronic newsletters, past issues of "Hipparchos", and proceedings of Conferences of Hel.A.S. The server is currently hosted by the University of Thessaloniki.

Astronomical Conferences & Schools in Greece during 2019

This issue includes brief presentations of ten conferences and schools, which took place in Greece during 2019, as well as of one from 2018, which due to an oversight is missing from the previous "Hipparchos". These meetings are:

- International Conference on Space Optics, Platanias, 9-12 October 2018.
- Exploring the Infrared Universe: The Promise of SPICA, Crete, 20-23 May 2019.
- Supernova Remnants II: An Odyssey in Space after Stellar death, Chania, 3-8 June 2019.
- 2019 Summer School for AstroStatistics in Crete, Heraklion, 18-21 June 2019.
- Supermassive Black Holes: Enviroment and Evolution, Corfu, 19-22 June 2019.
- Feedback and its Role in Galaxy Formation, Spetses, 25-29 June 2019.
- The 14th Conference of Hel.A.S., Volos, 8-11 July, 2019.
- Workshop on Computational Intelligence in Remote Sensing and Astrophysics, FORTH, 17-19 July 2019.
- Galaxy Formation and Evolution in a Cosmological Context, Spetses, 28 August - 5 September 2019.
- Crete III: Through dark lanes to new stars, Hersonissos, 23-27 September 2019.
- 14th Geant4 Space Users Workshop, Xylokastro, 21-23 October 2019.

1 International Conference on Space Optics

9-12 October 2018, Platanias

Te International Conference on Space Optics (ICSO – www.icso2018.org) took place in Platanias village near Chania during the period 9-12 October 2018. ICSO is the largest meeting worldwide of experts working in all disciplines of Optical, Optoelectronic and Photonic Technologies for Space Applications. It is organised biannually by the European and the Frence Space Agencies (ESA/CNES). This was the second time Greece hosted ICSO following the one in Rodos in 2010.

The purpose of ICSO is to bring together the Space Optics Community and exchange information and ideas on the Research, Development, Qualification and Flight Experience of using optical technologies for space missions. Technology experts meet Mission experts to address the lessons learnt from past developments and identify the next significant developments in employing lightwave technologies and techniques used in all types of Space Missions.

The conference attracted 450 attendees which is a new record for ICSO. Plenary Talks were delivered by Program/Project managers from ESA, NASA, JAXA and the Russian Space Research Institute. All the main, present and future, Space Missions involving Optical Instruments were presented as well as all the latest developments in optical technolo-

gies for Space. A highlight of the conference was the debriefing on the first measurements taken by ESA's "AEOLUS" mission which was launched on the 22nd August 2018. AEOLUS features as main Instrument a "Doppler wind LIDAR" to acquire profiles of Earth's wind on a global scale with near-real-time observations:

https://www.esa.int/Our_Activities/Observing_the_Earth/Aeolus/Introducing_Aeolus

This is the first LIDAR mission "Made in Europe" and as such everyone was eagerly expecting to see how the instrument behaves. Fortunately the results were very good confirming that European Industry masters the technology of spaceborne active optical instrumentation.

Of special interest were the 2 Special Guest Plenary Talks delivered by leading Greek scientists on:

- "*The Voyager mission 41 years after: Limits of the Solar System and Echoes from the Galaxy*" delivered by Stamatis Krimitzis, Chair of Science of Space at the Academy of Athens and Emeritus Head of the Space Exploration Sector of the Johns Hopkins Applied Physics Laboratory, and
- "*The Antikythera Mechanism: Decoding an astonishing 2000 years old astronomical computer*", delivered by John H. Seiradakis, Professor Emeritus, Aristotle University

These two Special Guest Plenary Talks captivated the audience offering a spectacular "Grand Finale" to the conference!

Nikos Karafolas

European Space Agency,
European Space Reserach and Technology Center
Noordwijk, The Netehrlands

2

Exploring the Infrared Universe: The Promise of SPICA

20-23 May 2019, Crete, Greece

Understanding in detail the origin and evolution of galaxies, stars, planets and life itself are fundamental objectives of astronomy. Although impressive advances have been made, our knowledge of how the first galaxies and stars formed, and how they evolve to into what we see around us today, is still far from complete. A major reason for this is that the birth and much of the growth of galaxies, stars and planets occurs in regions that are hidden by a thick blanket of dust – virtually inaccessible to the optical instruments that have been the tools of the trade since the invention of the telescope. A complete physical understanding of the processes that define our Universe is only possible with sensitive observations in the infrared, which can penetrate dust and reveal the inner workings of galaxies, star forming regions, and planet forming systems, over much of cosmic history.

https://www.spica2019.org

In May 2019, 164 experts from 21 countries, including 6 from Greece, convened in the island of Crete to discuss on the scientific program and technical developments of SPICA, a space infrared telescope for cosmology and astrophysics,

which is an M5 candidate mission for the Cosmic Vision program of ESA. Thanks to its large 2.5 m active cooled mirror bellow 8K, combined with a new generation of ultra-sensitive detectors, SPICA will offer the community a unique astronomical facility, able to cover the spectral range from 12 to 230 μm to unprecedented depths of a few 10^{-20} Wm^{-2} for spectroscopy (5σ) in 1 hour. This represents a gain in sensitivity of more than two orders of magnitude over both Spitzer and Herschel space telescopes, a gigantic leap in capabilities for exploring the Universe. As a consequence SPICA, if selected in 2021, is expected to revolutionize our understanding in all fields of astrophysics, from debris disks and planetary systems, to magnetic fields, star formation, active galactic nuclei and feedback, processes that shape galaxy evolution across cosmic time. Furthermore, it will complement current and upcoming facilities, such as JWST and ALMA.

All presentations of the conference are available online at:

https://spica-mission.org/?page_id=925

3

Supernova Remnants II: An Odyssey in Space after Stellar death

Chania, 3-8 June 2019

The international conference titled **"Supernova Remnants II: An Odyssey in Space after Stellar death"** explored the exciting recent observational and theoretical progress in the structure, evolution and physics of SNe and SNRs. The Institute for Astronomy, Astrophysics, Space Applications and Remote Sensing of the National Observatory of Athens (NOA), organized this meeting between June 3-8, 2019, at the «Minoa Palace Hotel», in Crete, Greece, with great success. The 193 distinguished scientists from 34 countries who participated in the conference truly exceeded our expectations, as they contributed presentations of a very high level and motivated many valuable scientific discussions. The goals of the meeting were understanding the evolution of SNRs and their interaction with interstellar gas, elucidating the physical processes that govern shock waves and relativistic plasmas, and inferring characteristics of supernova explosions from SNR observations. New understanding of the nature of supernova remnants and processes that occur there offers new insights into the role of SNRs in the structure and evolution of galaxies and the nature of supernova explosions.

Many new important results were presented such as (a) all the latest results about the famous Cassiopeia (Cas) A SNR (10 contributed talks and many posters, Fig.1) with surprising results, i.e. the existence of a reverse shock (Optical, often stationary where present – Fesen et al.; X-ray, moving back in W region – Vink et al.) and (b) new 3-D models of SNRs (i.e. First morpho-kinemaical model of VRO SNR – Derlopa et al.) and Pulsar-Wind Nebulae (PWNe, I,e, modelling PWNe and their magnetic fields – Olmi et al.).

Information about the scientific results can be found on the conference website:

http://snr2019.astro.noa.gr

under Program and Poster presentation.

Panos Boumis (SOC & LOC) & **Alceste Bonanos** (LOC)

Co-chairs

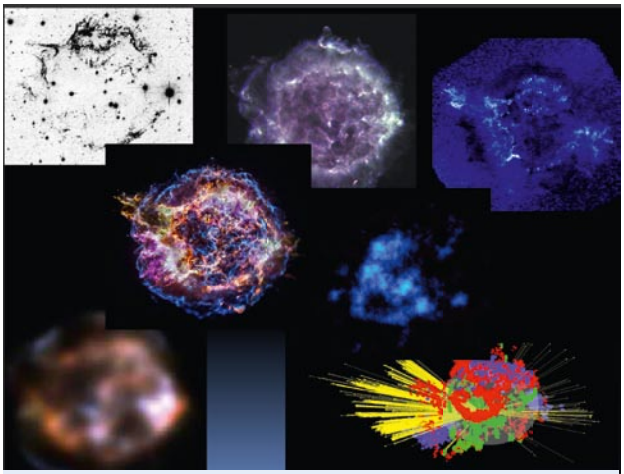

Figure 1: *Cas A images in different wavelengths and modelling presented by Fesen, Janka, Vink, Castro, Arias, Wongwathanarat, Holland-Ashford, Picquenot, Koo, Weil.*

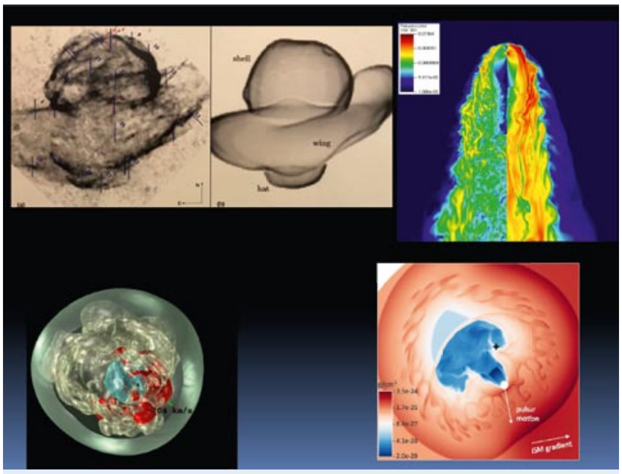

Figure 2: *3-D models of SNRs and PWNe presented by Derlopa, Olmi, Temim, Janka, Wongwathanarat, Orlado, Bochino, Milisavljevic etc.*

2019 Summer School for AstroStatistics

Crete, Heraklion, 18-21 June 2019

The first Astrostatistics Summer School was held at the Physics Department of the University of Crete (UoC, Heraklion), on June 18-21, 2019. Its goal was to guide advanced undergraduates, masters and graduate students, and early postdocs in the use of the latest statistical tools for the analysis of a wide variety of data.

Over the course of the week, participants worked with cutting-edge tools for the arsenal of the modern-day astronomer:

- Linear regression
- Hypothesis testing
- Bayesian statistics and Markov Chain Monte Carlo
- Machine learning, including regression, classification and clustering
- Time series analysis
- Deep learning

All teaching material is publicly available in the official site of the school:

http://astro.physics.uoc.gr/Conferences/Astrostatistics_School_Crete_2019/

The main highlight was the innovative approach we followed to provide a hands-on experience tailored to Astronomy. Each session had a theoretical introduction and was immediately followed by real-world applications through coding examples. The participants (in pairs) solved problems 'live' on computers provided by the Physics Department. This hands-on method allowed participants to quickly build up coding abilities while simultaneously serving as a practical reference in their future work.

Feedback suggests the school was both highly instructive and pragmatic within today's astronomical environment; the majority (92%) considered the sessions very/extremely useful, and of appropriate difficulty (70%). The attendants judged there has been a good balance between theory and workshops, and that Python codes were convenient and clear. Finally – in a survey carried out about 10 months later – 80% confirmed that the presented material and tools have been useful for their own research, while everyone reported the material aided with interpreting others' work.

The organizers plan to repeat the summer school in the coming years.

Any questions should be directed to:

astrostat@physics.uoc.gr

School instructors: ***Jeff Andrews*** *(University of Copenhagen),* ***Paolo Bonfini*** *(National Observatory of Athens),* ***Konstantinos Kovlakas*** *(UoC),* ***Grigorios Tsagkatakis*** *(UoC),* ***Davide Martizzi*** *(DARK - Niels Bohr Institute), and* ***Grigoris Maravelias*** *(National Observatory of Athens).*

This school has received funding from the EU Horizon 2020 grant #691164 (ASTROSTAT).

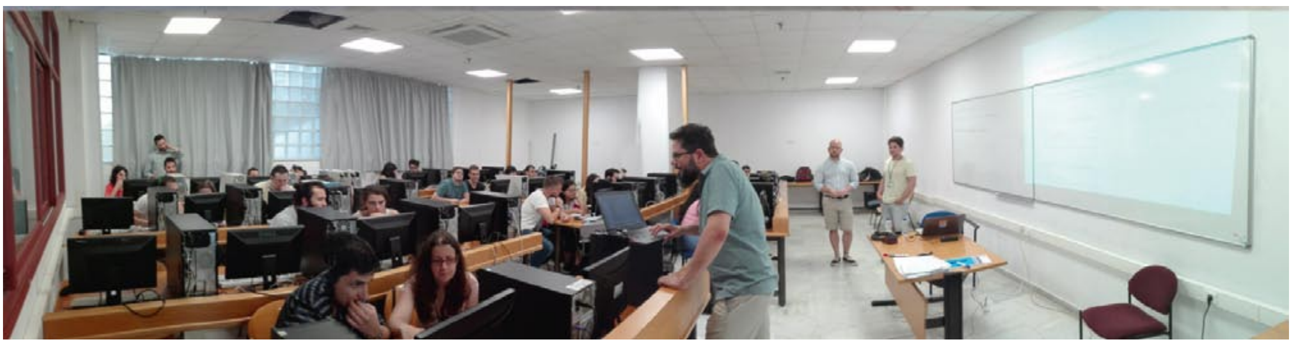

5

Supermassive Black Holes: Enviroment and Evolution

Corfu, 19-22 June 2019

The X-ray Astronomy group of the Institute of Astronomy Astrophysics Space Applications and Remote sensing (IAASARS) has organised an Astronomy conference on Supermassive Black Holes in Corfu last June. The group regularly organises a series of conferences in X-ray Astronomy and Cosmology every four years with the first one organised 20 years ago. The conference has been organised by the X-ray Astronomers of IAASARS I. Georgantopoulos, A. Georgakakis, E. Koulouridis and A. Akylas with the help of the director of IAASARS and the president of the National Observatory of Athens. The effort of many postdoctoral research associates and research students of our group was a key factor in the success of the event. The conference took place in the historical building of the Rectory House of the Ionian University. The building hosted the first University in Hellas, the Ionian Academy that started its operations in 1824.

The conference focused on the environment , the evolution of the supermassive black holes as well as their interaction with their surrounding galaxies and clusters of galaxies. The aim was to discuss the most recent multi-wavelength observations and compare them with simulations and observations. The discovery space that opened up with current missions such as XMM , Chandra, Spitzer and Herschel but also with ground based facilities such as VLT, ALMA, has been thoroughly explored in this conference. The new horizons that open up in the studies of supermassive black holes with the new missions eROSITA, XARM, JWST and ATHENA were a primary part of this meeting. One of the many conference highlights included the talk by F. Nicastro (Rome Observatory) on the first detection of the warm-hot intergalactic medium (WHIM). The warm–hot intergalactic medium refers to a sparse, warm-to-hot (10^5 to 10^7 K) plasma that exists in the intergalactic space and contains about 40–50% of the baryonic content of the Universe. The WHIM discovery only became possible with ESA's XMM X-ray mission observing the light of a distant quasar in absorption by this warm-hot diffuse gas.

The conference has been attended by about 120 participants from many countries around the world. Most participants came from Italy and then from the United Kingdom, United States, Chile and China. Among them more than 20 Greek astrophysicists, coming from Research Institutes and Universities both in Greece and abroad. This demonstrated the strong presence of Greek scientists in this exciting field of astrophysics.

I. Georgantopoulos

The conference photograph outside the historic Ionian Academy building under the flying lion of Venice

6

International Conference

Feedback and its Role in Galaxy Formation

25-29 June 2019, AKSS, Spetses, Greece

On 25-29 June 2019 a hundred researchers working on feedback from supernovae and active galactic nuclei (AGN) met at the Anargyrios and Korgialenios School of Spetses (AKSS) for a conference on "Feedback and its Role in Galaxy Formation". Cattaneo (2019, Nature Astronomy, vol. 3, p. 896-897) has reported on the main new scientific results emerged during the meeting. Here are the main highlights.

The conference started from the observational evidence for stellar and AGN feedback in the Milky Way and other nearby galaxies. The consensus that in massive spirals the ratio of the outflow rate to the star-formation rate is never much larger than one to ten was not perceived as a challenge for galaxy formation models. The absence of detected outflows at lower masses (Alice Concas) is a potentially more serious issue.

The meeting continued with a long series of talks on hydrodynamic simulations from interstellar-medium scales (Chang-Goo Kim, TIGRESS) to cosmological one (Joop Schaye, EAGLE). Thales Gutcke presented the first cosmological zoom simulations with individual supernovae. Benjamin Keller proposed that outflows are entropy-driven (buoyant) rather than energy-driven. Lilian Garratt-Smithson showed that, once supernovae carve low-density chimneys in the gas, stellar winds and high-mass X-ray binaries can keep them open and maintain the outflows active.

Dylan Nelson (TNG50), Daniel Anglés-Alcazar (FIRE), Edouard Tollet (NIHAO) and Joop Schaye (EAGLE) showed that different groups are converging on a coherent picture. Neal Katz cautioned that none of these simulations are able to resolve the multiphase structure of galactic winds. Their results appear to converge simply because all groups have tuned their subgrid physics reproduce the same data.

A session on chemical evolution concluded the first half of the conference, mainly on stellar feedback. In the second half, where AGN feedback was the main topic. Kalliopi Dasyra talked about the excitation of the molecular gas in winds and its impact for wind detections and masses. Serena Perrotta showed that extremely red quasars can be explained as a short-lived blow-out phase during which the pressure of trapped infrared radiation boosts galactic outflows. Asa Bluck reported that the mass of the central black hole is an excellent predictor of quiescence, in agreement with the observation that the massive galaxies where feedback has failed to prevent star formation are all spirals (Lorenzo Posti).

The conference ended with a series of talks on early-type galaxies and clusters. Luca Ciotti and Feng Yuan discussed episodic AGN feedback. Dong-Woo Kim remarked that the

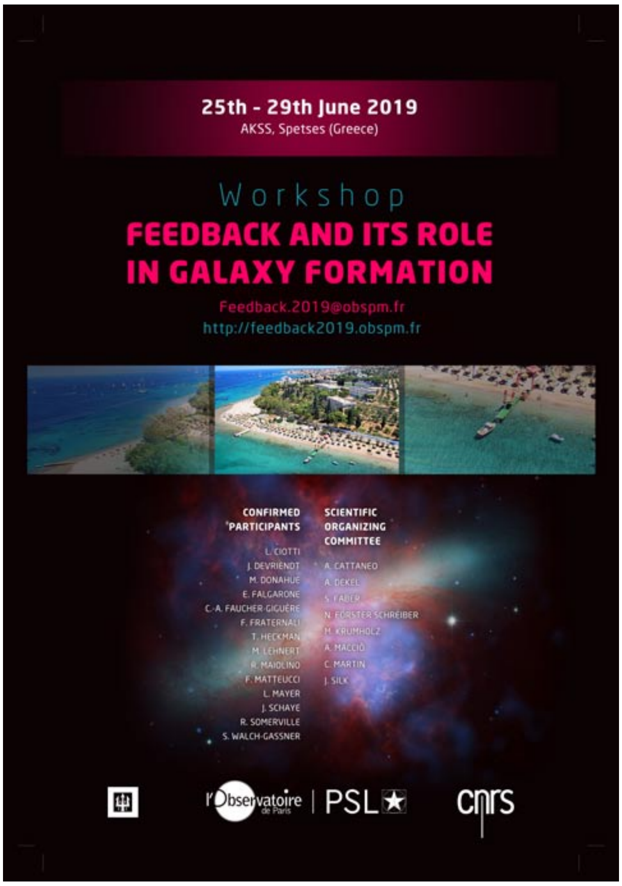

X-ray profiles of early-type galaxies are more complex than those of galaxy clusters because the effects of feedback are more pronounced. Julie Hlavecek-Larrondo presented new evidence that the intracluster medium is maintained in thermal equilibrium by the balance of radiative cooling and AGN heating, but one of the meeting's greatest novelties was the mounting consensus for a precipitation scenario in which the intracluster medium becomes multiphase when the cooling time becomes shorter than about ten freefall times (Mark Voit, Arif Babul, Megan Donahue).

Scientific Organising Committee:
A Cattaneo, A Dekel, S M Faber, N Förster Schreiber, M Krumholz, A V Macciò, C Martin, J Silk

The talks can be found at:

http://feedback2019.obspm.fr/index.php/programme

7

The 14th Hellenic Astronomical Conference

8-11 July 2019, Volos

The 14th Conference of the Hellenic Astronomical Society took place in Volos, from 8 to 11 July, 2019. Despite the fact that national elections were unexpectedly announced and held just at the date initially planned for the opening of the conference, it has been attended by close to 100 registered participants. A total of 86 oral papers were delivered as well as a number of posters. We underline the plenary talks that have been given by S. Antiochos, NASA/Goddard Space Flight Center, MD, USA, E. Athanassoula, Aix Marseille Université, CNRS, LAM Laboratoire d' Astrophysique de Marseille, Marseille, France, N. Stergioulas, Aristotle University of Thessaloniki, Greece and G. Gilmore, University of Cambridge, Institute of Astronomy, UK. The opening talk was given by N. Prantzos, Institut d' Astrophysique de Paris, France, while three more talks for the broad public have been presented by Th. Economou, University of Chicago, USA, C. Gontikakis and P. Patsis, Research Center for Astronomy and Applied Mathematics of the Academy of Athens, in the frame of the celebrations of the 100th anniversary of the International Astronomical Union (IAU). The conference has been supported by the University of Thessaly, the Academy of Athens and the National Observatory of Athens. The local organization of the conference has been managed by Hel.A.S. members, with a major contribution by members of the Society of Space and Astronomy, based in Volos, under the coordination of its president L. Zachilas.

8

International Workshop on Computational Intelligence in Remote Sensing and Astrophysics (CIRSA)

July 17-19, 2019, FORTH, Heraklion, Crete

The objective of the International Workshop on Computational Intelligence in Remote Sensing and Astrophysics (CIRSA) was to bring together scientists from different disciplines including astronomy, environmental engineer, and computer science for addressing the challenges associated with the analysis of the vast amount of observations acquired by modern instruments, both in Earth Observation as well as in deep space imaging. The core theme involves the use of cutting computational intelligence tools including deep machine learning models, in order to address crucial scientific questions such as:

- Machine learning in gravitational lensing cosmology
- Automated characterization of supernova and galaxy morphology
- Advances in hyperspectral imaging and learning
- Deep learning in satellite image processing
- Big Data from Space and intelligent decision making

The workshop was organized by Grigorios Tsagkatakis (ICS-FORTH), Jean-Luc Starck (CEA), Vassilis Charmandaris (IA-FORTH), and Panagiotis Tsakalides (ICS-FORTH) and took place at the premises of FORTH.

The workshop featured numerous international speakers: Dr. Shirley Ho from the Center for Computational Astrophysics in NY, Prof. Enrico Magli from the Politecnico di Torino, Dr. Athanasios Rontogiannis and Dr. Haris Kontoes, from the National Observatory of Athens, Dr. Nektarios Chrysoulakis and Dr. Kostas Tassis from FORTH, Dr. Georgios Vernardos from the University of Groningen, and Prof. Konstantinos Karantzalos from NTUA, among others

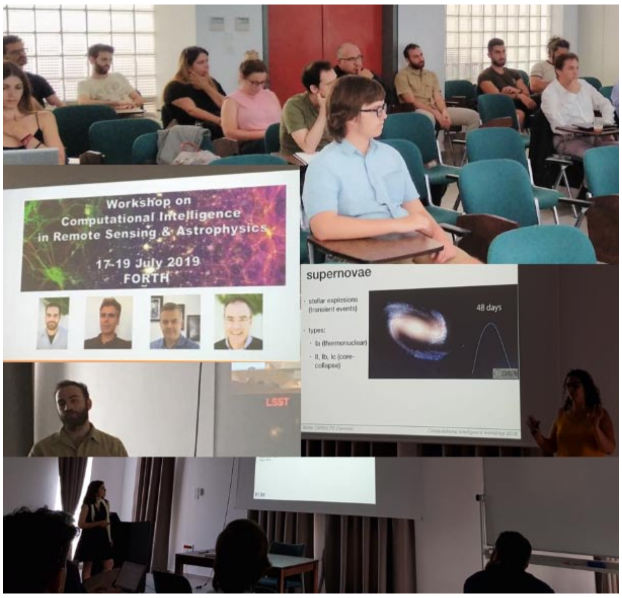

The website of the conference is:

http://spl.edu.gr/index.php/CIRSA

9

The 4th Summer School
Galaxy Formation and Evolution in a Cosmological Context

28 August - 5 September 2019, AKSS, Spetses, Greece

The fourth Observatoire de Paris/LAM Summer School "Galaxy Formation and Evolution in a Cosmological Context" took place at the Anargyrios and Korgialenios School of Spetses (AKSS) from 28 August to 5 September 2019. The 42-hour school aims to assist PhD students to bridge the gap between master courses and the knowledge required to lead an autonomous research project.

Andrea Cattaneo, currently at the Observatoire de Paris, organised the first summer school in 2013, when he was a lecturer at the Laboratoire d'Astrophysique de Marseille (LAM). The school is biennial and has been hosted by the AKSS since 2017. In 2019 the school trained 24 PhD students, 1 undergraduate and 1 postdoc from 10 different countries. Their provenance included world-leading institutions such as Caltech, the University of Oxford and the Max Planck Institute for Astrophysics.

The school has a core programme centred on four courses:

1) star formation and its implications for the spectral and chemical evolution of galaxies (Samuel Boissier, LAM),
2) galaxy evolution in deep surveys (Olivier Le Fèvre, LAM),

3) cosmological hydrodynamic simulations (Julien Devriendt, Oxford), and
4) semianalytic models of galaxy formation (Andrea Cattaneo).

Unfortunately, serious illness prevented Olivier Le Fèvre from delivering his lectures personally at the fourth summer school.

In addition to these recurrent topics, the school also develops a new theme each time. In 2017 it was the first stars and the epoch of cosmic reionization (Andrea Ferrara, Scuola Normale Superiore, Pisa, Italy). In 2019 it has been galaxy clusters with an emphasis on the exciting discovery of protoclusters at high redshift. The course on clusters and protoclusters has been taught by Gary Mamon (Institut d'Astrophysique de Paris) and Olga Cucciati (Istituto Nazionale di AstroFisica, Italy).

The slides of all lectures can be found at:

http://galaxyformationschool2019.obspm.fr

10

Crete III: Through dark lanes to new stars Celebrating the career of Prof. Charles Lada

Crete, September 2019

The Crete NATO Advanced Study Institutes on Star Formation in 1990 and 1998 (Crete I and Crete II, respectively), organized by Charles Lada and Nick Kylafis, were landmarks in the development of the star- and planet-formation community. Many of the attendants of these schools are now well-established researchers across the world, pushing the boundaries of the field with a new generation of telescopes and simulations. It seemed appropriate to return to Crete in 2019 to organize Crete III and celebrate the legendary Star Formation schools and the career of Prof. Charles Lada.

The Crete III conference took place on the island of Crete in September 2019 and counted about 100 participants from across the world, including many star formation specialists as well as students. About 50 colleagues and collaborators of Prof. Lada, who could not be present, sent written and video messages with stories in what was one of the highlights of the meeting. Of all the 10 PhD students of Prof. Lada, from the early eighties to today, only one could not be present. The tone of the meeting was celebratory, with presentations from across several generations of astronomers on the main topics of research of Prof. Lada, namely:

– Molecular clouds
– Dense cores
– Disks and outflows
– YSO classification
– Embedded clusters
– Star formation rates and efficiencies in the Milky Way and beyond

The promise to return to this enchanted island for Crete IV and organize Star and Planet Formation school in the 2020s is in the air. Stay tuned!

João Alves

11

14th Geant4 Space Users' Workshop

Xylokastro, 20-23 October 2019

The 14th Geant4 Space Users' Workshop (G4SUW) was coorganized by the European Space Agency, Stanford/SLAC and the University of Athens in Xylokastro, Greece, on 20-23 October 2019 (https://indico.esa.int/event/304/). As always, G4SUW focused on new results on space radiation interaction with components, sensors and shielding analysis, as well as on Geant4-based tools and developments applicable to space missions.

More than 40 scientists participated in this Workshop, to discuss recent developments in the usage of physics simulation toolkits for space applications, including not only GEANT4, the standard tool for such simulations, but several similar other software packages.

The workshop started with the status reports of various upcoming national/international projects, including European (ESA), American (JPL), Japanese (JAXA) and Chinese (CSA). For example, the intense Jovian radiation Environment is currently actively studied and simulated due to upcoming missions headed to our solar system's giant, namely ESA's Jupiter Icy moons Explorer (JUICE) and NASA's Europa Clipper.

Further projects discussed include ESA Cosmic Vision L-class mission ATHENA (Advanced Telescope for High Energy Astrophysics), NASA's Star-Planet Activity Research CubeSat (SPARCS) and Imaging X-ray Polarimetry Explorer (IXPE) and JAXA's MMX (Martian Moons Exploration). The increasing complexity of such scientific future missions results in increasingly sophisticated tools (which were also presented), such as AREMBES (Athena Radiation Environment Models and x-ray Background Effects Simulator) – an ESA project that foresees the development of a software simulator based on Geant4, capable of addressing all the background issues that the ATHENA mission will experience during its lifetime.

Another major theme of the workshop was the presentation of new tools that can interface between the physicist and the engineer. Tools for the easy construction of geometries, the python API of GEANT4, Geant4Py, the prediction of wear of electronics in space (TRADCARE) are some of the examples. Last but not least, ESA's SPENVIS (Space ENVironment Information System) is an online free interface to various Geant4-based tools that can be used for supporting scientific studies related to the characterisation of the space environment and its effects. It includes an implementation of GRAS (Geant4 Radiation Analysis for Space), a specialized tool developed by ESA. Such tools may support the prediction of space environment impacts on human tissue, another fast-evolving topic.

In this year's G4SUW there was a particularly strong Greek component. First through the study of the MIDAS dosimeter/radiation monitor, a highly miniaturized ASIC radiation detector developed under contract for ESA. And also through the presentations of G4G, the "Geant4-based Particle Simulation Facility in Greece for Future Science Mission Support", an ESA project implemented by a consortium including IASA (University of Athens), NCSR "Demokritos", National Technical University of Athens, and University of Ioannina, which designs, develops and tests software and documentation within a framework provided by ESA.

Back issues of Hipparchos

Hipparchos is the official newsletter of the Hellenic Astronomical Society. It is distributed by post to the members of the society. You can download back issues from: **http://www.helas.gr/news.php**